博士論文

Studies on surface lubricated honeycomb films prepared by self-organization process for oil-water separation

（表面潤滑層を持つ自己組織化ハニカムフィルムによる油水分離に関する研究）

CHEN BIHAI

陳 碧海

令和 4 年

CONTENTS

ABSTRACT

The separation of oil and water is important for solving various water-related problems, such as industrial wastewater purification. The separation of oil and water by gravity is an important technology and porous membranes are widely applied in oil-water separation. The wettability control of the membrane to oil and water is very important. The hydrophobic-oleophilic membranes can be used when the density of oil (ρ_{oil}) > 1 and the hydrophilic-oleophobic membranes can be used when $\rho_{oil} < 1$ in gravity-driven system.

A honeycomb-like polymer porous membrane, which has uniform pore sizes can be prepared by casting polymer solution under humid conditions and templating condensed water droplets as templates. A perforated honeycomb membrane can be fabricated by this “breath figure” technique and it has hexagonally-packed pores, and those have connected each other inside of the film. This perforated honeycomb membrane has ideal structure for oil/water separation membranes.

In this thesis, this is the first report about application of HC films to liquid separation membranes and variety of applications, including energy-saving separation and purification and removal of oil spills, are expected. Also, smart separation membranes can be realized to control oil and water separation selectively by introduction stimuli-responsive properties to the HC films, which have already reported in the previous literatures.

Relying on the lubricating layer as a transition switch, I use the same amphiphilic membrane to exhibit both hydrophilic-oleophobic and oleophilic-hydrophobic wettability, which allows the membrane to separate oil and water in gravity-driven system no matter $\rho_{oil} > 1$ or $\rho_{oil} < 1$.

It is known that hydrophilic micro-structured surfaces repel oil droplets, which is seen in a natural surface structure of a fish scale. The honeycomb film treated by UV-O_3 becomes hydrophilic and underwater oleophobic which could use for

oil-water separation. And the transparency of hydrophobic honeycomb and pincushion films will be significantly improved underwater.

The hydrophobic honeycomb film can also separate oil and water with oil-removing method. There is an interesting phenomenon that some spherical droplets come out from the films when measure the decane contact angle underwater. After dyeing the decane red, it can be known that the droplets come out from the films are bubbles. And through the analysis of surface tension changes, it can be obtained that the decane cannot spread but are absorbed in the honeycomb film.

CHAPTER 1. GENERAL INSTRUCTION AND LITERATURE REVIEW

1.1 CONTAMINATION OF OIL-WATER MIXTURE AND CONVENTIONAL SOLUTIONS

The separation of oil and water is an important technology for solving a wide range of water-related problems such as purification of industrial wastewater, [1-4] oil leakage from ships, [5-8] and securing drinking water in developing countries. [9-12] The treatment of crude oil and organics, as well as the treatment of a large amount of oily wastewater produced by industries, urgently requires a high-performance oil-water separation material.

Conventional treatment methods for large-scale oil spills at sea include using sorbents, [13,14] in-situ burning method, [15,16] using dispersants, etc. [17,18] Common sorbents include porous materials such as corn stalk. [14] However, the selectivity of such conventional porous materials is poor, and large amounts of moisture are often present in the adsorbed oil. Not only does this reduce efficiency, but it also makes it more difficult to reuse the recovered oil. In-situ burning significantly reduces the oil content in the water, but results in a waste of crude oil. In addition, the toxic and harmful gases produced during the combustion process will also cause secondary pollution to the environment. At the same time, the release of a large amount of carbon dioxide gas is also contrary to the concept of energy conservation and emission reduction advocated by the international community. [15] The chemical dispersant degradation method cannot fundamentally eliminate the leaked oil and organic matter, and many chemical dispersants themselves are toxic and harmful to the environment, which will cause more serious secondary pollution. [17]

The conventional separation methods of oily wastewater discharged from our daily life and industries include centrifugal separation, [19] gravity separation, [20-23] and electrolysis separation, [24,25] etc. In a standard gravity separator, as shown in Figure 1-1, oil droplets rise to the surface after a sufficient residence time to form a fluid suspension layer, which can then be recovered by skimmers, pumps, or other methods. This method requires long-term storage of a large

amount of sewage, the storage cost is greatly increased, and the efficiency is low. Although most processes of this method have been applied to practical oil-water separation, the disadvantages of low separation efficiency, slow separation speed, and high cost limit the development of these traditional processes.

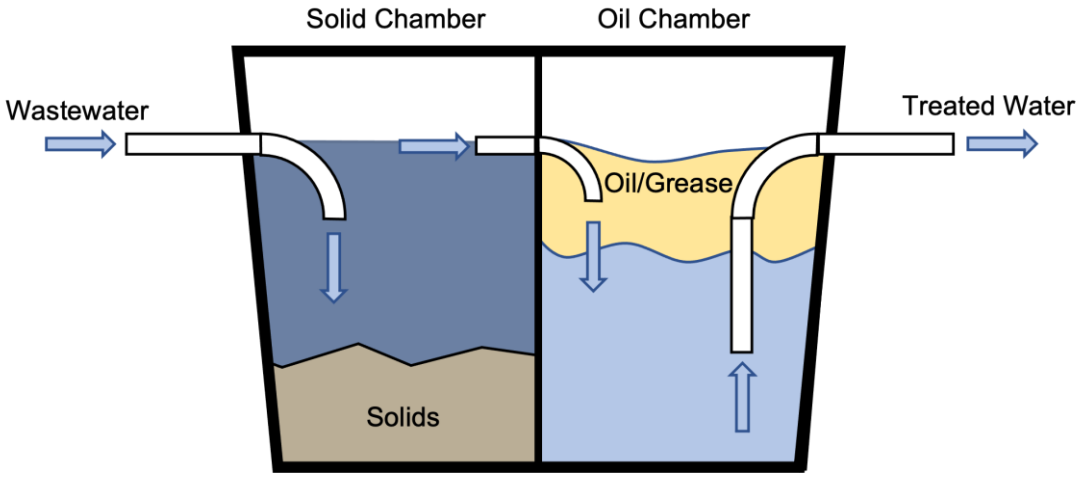

Figure 1-1. Standard gravity oil/water separator.

Membrane separation is expected to be a relatively simple and efficient oil-water separation method. [26-35] In membrane separation, the properties of the separation membrane, such as pore size and wettability, determine the efficiency and range of applications. Therefore, high-performance oil-water separation membranes are being actively researched and developed. Obviously, controlling the pore size and surface wettability of the oil-water separation membrane is a key issue.

1.2 BIOMIMETIC SUPERHYDROPHOBIC MATERIALS

Over billions of years of evolution, organisms have developed excellent functions and advanced structures. By observing natural phenomena and the characteristics of organisms, people get a lot of inspiration. [36-40] By mimicking the composition, structure and function of natural organisms, new material design ideas can be obtained, which will help to develop new functional and high-performance materials, so as to solve problems encountered in life and production and promote social development and progress. [41-48]

The lotus leaf is an aquatic plant that lives in muddy swamps and ponds, where the lotus leaf has evolved a unique self-cleaning function. It is well known that the water droplets that fall on the lotus leaf will form approximately spherical water droplets, roll on the surface of the lotus leaf without infiltrating the lotus leaf, and take away the dust on the surface of the lotus leaf. [37] A water strider is an aquatic insect that can float on water on its four legs. [49]

Superhydrophobic surfaces having hierarchic surface structures have been developed using water repellent lotus leaves [37] and insect wings as models. [50-52] The common features of lotus leaf surface and water strider legs are superhydrophobicity and superoleophilicity. [52,53] By studying the composition and structure of the surface of lotus leaves and water strider legs [37,50], the researchers found that superhydrophobic surfaces can be prepared by combining micro-nano roughness structures with low surface tension substances. [53,54]. Because most materials are oleophilic, the fabrication of materials with the superhydrophilic property is of great significance for oil-water separation.

1.3 WETTABILITY AND SURFACE TENSION

Surface tension is the tendency of a fluid surface to shrink to its minimum surface area. The existence of surface tension allows some insects that are denser than water to float and slide on the surface. [49]

Laplace pressure is the origin of the pressure at the curved liquid interface. At liquid–air interfaces, the liquid molecules are replaced by the gas for the attraction of liquid molecules to each other greater than the molecules in the air. So, the attractive force is unbalanced, and the liquid will have a tendency to spontaneously turn inward, and the resultant force will point to the inside of the droplet. This is the origin of surface tension of the liquid. The phenomenon of surface tension can be regarded as a surface defect, and the surface has more energy than the interior. So, from the energy point of view, according to the principle of minimum energy, atoms will spontaneously tend to the interior of matter rather than the surface.

The pressure difference between the inside and the outside of a curved surface caused by surface tension could be calculated by the Laplace equation

$$\Delta P = \frac{2\Upsilon}{R} \qquad (1-1)$$

where Υ is the surface tension, R is the principal radii of curvature.

The wettability of material is macroscopically a process in which a fluid replaces another fluid on a solid surface. The spreading ability of a fluid on a solid surface is called wettability. The stronger the spreading ability, the better the wettability of the fluid on the solid surface. The spreading coefficient S can be defined as [56]

$$S = -(\Upsilon_{SL} + \Upsilon_{LG} - \Upsilon_{SG}) \qquad (1-2)$$

where Υ_{SL} is the surface tension of liquid and solid, Υ_{LG} is the surface tension of liquid and gas, Υ_{SG} is the surface tension of solid and gas. $S \geq 0$, the liquid can spread on the solid surface, $S < 0$, the liquid cannot spread on the solid surface.

The relationship between surface tension and wettability is shown in the Figure 1-2. Because of the relatively high attraction of water molecules to each other through hydrogen bonds, water has a higher surface tension (72.8 millinewtons per meter at 20 °C) than most other liquids.[55]

When the surface tension of solid surface is high enough, it exhibits hydrophilic and oleophilic properties. When the surface tension of solid surface is low enough, it exhibits hydrophobic and oleophilic properties.

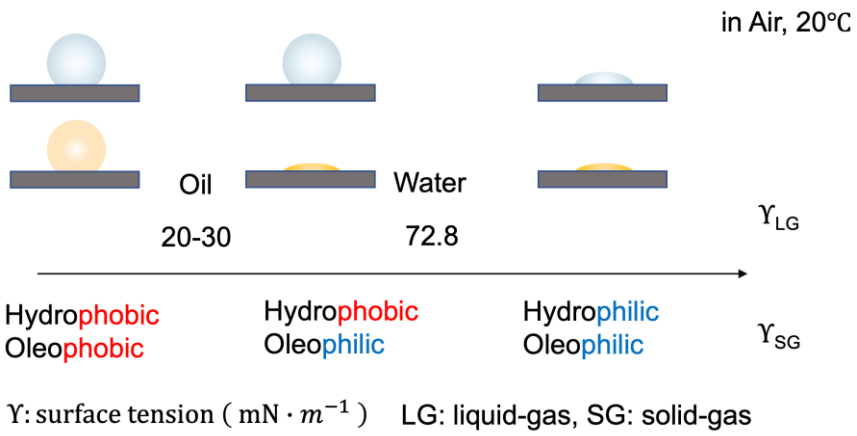

Figure 1-2. The relationship between surface tension and wettability.

Contact angle can be indicated by Young's equation [57]

$$\cos\Theta = \frac{\gamma_{SG} - \gamma_{SL}}{\gamma_{LG}} \qquad (1-3)$$

where γ_{SG} is the surface tension between solid and air, γ_{SL} is the surface tension between solid and liquid, γ_{LG} is the surface tension between liquid and air. (Figure 1-3)

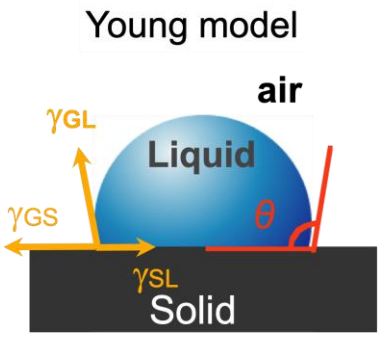

Figure 1-3. Scheme of Young model.

Young's equation only applies to ideal smooth surfaces. However, in practice, the contact angle of a rough surface is different from the intrinsic contact angle.

In order to explain this phenomenon, Wenzel established a model,[58] assuming that the liquid thoroughly wets the rough structure of the real surface and fills

the gaps and grooves in the rough surface (Figure 1-4), thereby affecting the wettability and contact angle of the material (Figure 1-5).

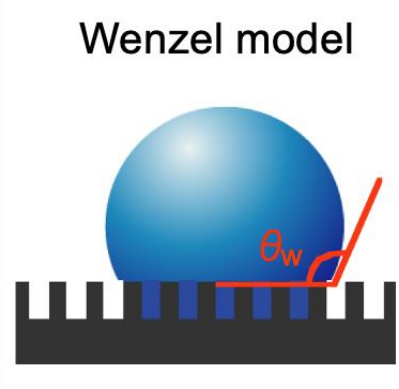

Figure 1-4. Scheme of Wenzel model.

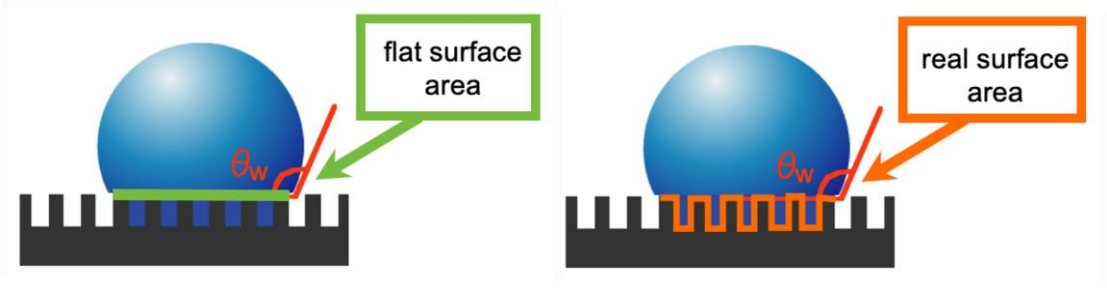

Figure 1-5. The flat surface area of apparent contact surface and real surface area of Wenzel model.

The Wenzel equation introduces roughness to modify the young equation. By the Wenzel model, contact angle (Θ_w) can be calculated by Wenzel equation.

$$\cos\Theta_w = r\cos\Theta \qquad (1-4)$$

where r is the roughness and $r = \frac{real\ surface\ area}{flat\ surface\ area}$.

From the Wenzel model, it can be known that for a hydrophobic surface that the contact angle larger than 90°, increasing the roughness of the material can make the surface more hydrophobic, and for a hydrophilic surface the contact angle less than 90°, increasing the roughness of the material makes the surface more hydrophilic. In other words, increasing the roughness of the material will

make the hydrophobic surface have lower surface tension and make the hydrophilic surface have higher surface tension.

The Wenzel model is suitable for chemically homogeneous surfaces but not for complex multiphase surfaces.

Another model established by Cassie and Baxter,[59] this model assumes that when a droplet contacts a rough surface, the surface that the liquid contacts is composed of two components with different wettability (Figure 1-6). In this model, the contact angle (Θ_C) of a surface composed of two components is given by a formula based on the fraction of each component.

$$\cos\Theta_C = f_1 \cos\Theta_1 + f_2 \cos\Theta_2 \qquad (1-5)$$

where f_1 and f_2 are the fractions of the two components, and Θ_1 and Θ_2 are the contact angles of a liquid on a flat surface composed of components 1 or 2.

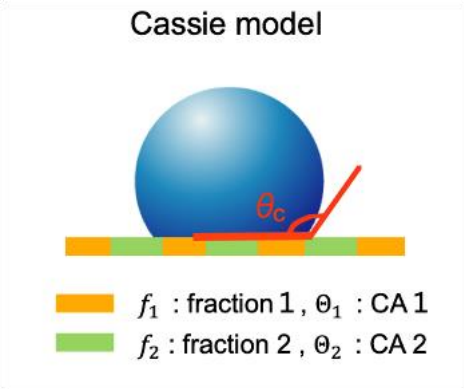

Figure 1-6. Scheme of Cassie model.

A typical application is when the second part is air. After the liquid contacts the rough surface, it does not completely wet the real surface, but has air in the grooves of the rough structure. (Figure 1-7).

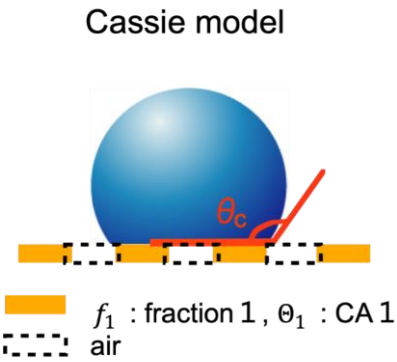

Figure 1-7. Scheme of Cassie model when the second part is air.

Because $f_1 + f_2 = 1$, equation 1-3 can be transformed into

$$\cos\Theta_C = f_1 \cos\Theta_1 + f_1 - 1 \qquad (1-6)$$

According to the Cassie equation (1-6), for hydrophobic surfaces, the smaller the contact area between solid and liquid (the smaller f_1), the better the hydrophobicity of the solid surface.

1.4 OIL-WATER SEPARATION METHOD WITH POROUS MATERIALS

1.4.1 APPLICATION OF HYDROPHOBIC AND OLEOPHILIC MATERIALS IN OIL-WATER SEPARATION WITH OIL-REMOVING METHOD

Inspired by natural organisms, a large number of artificial superhydrophobic materials have been prepared for oil-water separation. [60-67] To prepare superhydrophobic surfaces, the methods include roughening the surface of low-surface-energy substances and coating the low-surface-energy substances on the rough surface.

Feng L et al. [60] used polyvinyl acetate as a binder, polyvinyl alcohol as a dispersant, and sodium dodecylbenzene sulfonate as a surfactant to disperse polytetrafluoroethylene (PTFE) in water to form an emulsion. After dedusting, cleaning and drying the stainless-steel mesh with a pore size between 30 to 420 μm, the PTFE emulsion was sprayed on the stainless-steel mesh by drying air, and then the sprayed stainless-steel mesh was heated at 350 °C for 60 min

to remove the stickiness. After binding agent, dispersant and surfactant, PTFE covered stainless steel mesh was obtained.

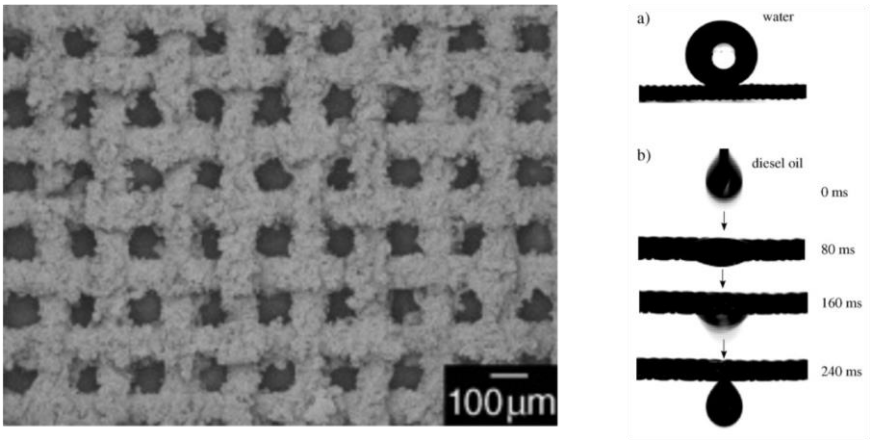

Figure 1-8. SEM images of the coating mesh film prepared from a stainless-steel mesh coated with PTFE. a) The water droplet can be repelled on the mesh b) The oil droplet can quickly pass through the mesh. [60]
(Reproduced with permission, Copyright © 2004 WILEY-VCH Verlag GmbH & Co. KGaA, Weinheim)

Through scanning electron microscope observation, the holes of the stainless-steel mesh covered with PTFE are not blocked by PTFE, and the surface of the stainless-steel mesh is covered with PTFE, and the morphology is spherical and block. The surface of the PTFE microspheres was observed under a high magnification scanning electron microscope, and it was found that the morphology of the PTFE microspheres was similar to that of a golf ball, and there were a large number of pores with a diameter of 71±8nm evenly and tightly arranged on the surface of the sphere (Figure 1-8). Under the combined action of the micro-nano hierarchical structure formed by PTFE on the surface of the stainless-steel mesh and the low surface energy of PTFE, the stainless-steel mesh is superhydrophobic and superoleophilic and the contact angle for water on this film is greater than 150°, and for diesel oil it is 0°.

The superhydrophobic and superoleophilic material of the stainless-steel mesh covered with PTFE enables it to separate oil and water. As shown in Figure 1-8, the water droplets can stay on the surface of the stainless-steel mesh, and

the diesel oil droplets Then it leaks from the stainless-steel mesh, so that the oil-water mixture can be separated.

Feng L et al. pioneered the use of superhydrophobic and superoleophilic two-dimensional network materials for oil-water separation. Since then, many two-dimensional network materials such as superhydrophobic and superoleophilic metal meshes covering polymers or polymer composites have been developed for oil-water separation.

1.4.2 APPLICATION OF HYDROPHILIC AND OLEOPHOBIC MATERIALS IN OIL-WATER SEPARATION

Although various hydrophobic and lipophilic materials have been developed and proven to be very promising in selective oil-water separation, under gravity systems, only oils with densities greater than water can be selectively separated. This is because a water barrier is formed between the filter material and the oil layer that is less dense than water, hindering the filtration process.[68] In contrast, hydrophilic and oleophobic materials that can selectively remove water can avoid the problem.

From the viewpoint of surface tension (Figure 1-9), it is theoretically difficult to prepare materials that exhibit both hydrophilic and oleophobic properties because the surface tension of water is usually higher than that of oil. [69]

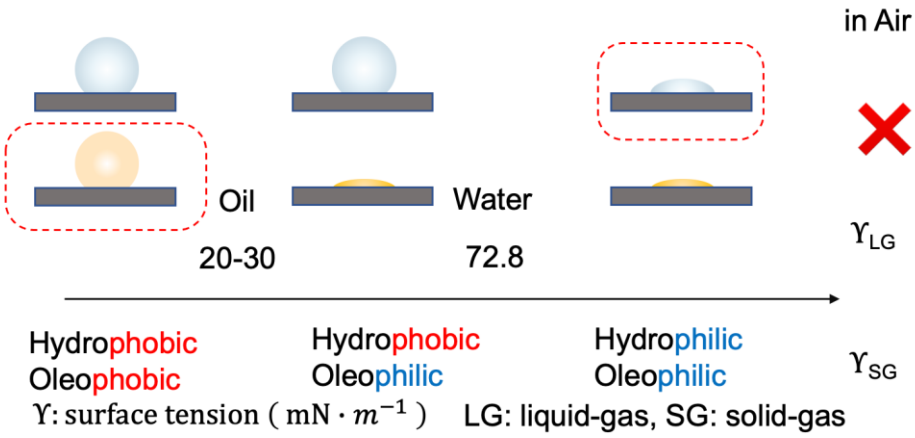

Figure 1-9. Scheme of wettability and surface tension. Hydrophilic and oleophobic surface cannot be prepared theoretically.

So far, only a few hydrophilic and oleophobic materials have been reported. They are generally polymers composed of hydrophilic and oleophobic components. The oleophobic component will make the surface oleophobic without contact with water. However, when the polymer surface is in contact with water, the interaction of the hydrophilic groups with polar water molecules can cause the rearrangement of the polymer chains, so that the hydrophilic moieties are located at the solid/liquid interface, thereby achieving hydrophilicity. In other words, these materials are water responsive. [70]

1.4.3 OIL LUBRICATING LAYERS

Aizenberg *et al.* developed a slippery liquid-infused porous surface (SLIPS) inspired by Nepenthes pitcher plants. [71,72] A water-immiscible lubricating organic liquid was trapped in the surface textures to have a molecularly smooth surface with low water contact angle hysteresis. This methodology is applicable to various inexpensive and low surface energy structured materials like Teflon and epoxy resin. Driven by capillary attraction, lubricant migrated from the wetting ridge and the substrate's texture to the frozen droplet's surface. In this case, lubricant could be gradually depleted during deicing or defrosting cycles and SLIPS failed in lubricating.

Recently, Aizenberg *et al.* reported that the thermodynamically stability of SLIPS could be improved by employing a closed-cell architecture. [72] The lubricants could be firmly locked in the structures and the lubricant-infused layers demonstrated excellent thermodynamically stability of over 9 months vertical storage.

1.4.4 FISH SCALES AND WATER LUBRICATING LAYERS

Fish scales are composed of calcium phosphate, protein, and a thin layer of mucus that leads to their hydrophilic behavior. [73-78]

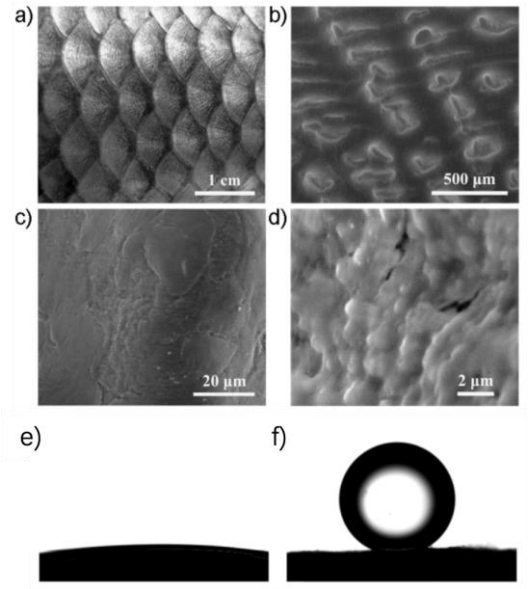

Figure1-10. Underwater superoleophobicity of fish scale surface and oil contact angle. [75] (Reproduced with permission, Copyright © 2009 WILEY-VCH Verlag GmbH & Co. KGaA, Weinheim)

Water can be trapped in the rough microstructure of fish scales, and the surface, after holding water, can form an aqueous lubricating layer which can repel air bubbles and oil droplets to keep the fish body clean in water. The introduced layer of water decreases the contact area between the oil and the surface of the scale and therefore decreases the adhesion force between them, giving the scale its oleophobic properties, as shown in Figure 1-10. This leads us to the concept of biomimetic underwater oleophobic surfaces that use microstructure and surface chemistry to control the interaction between solid surfaces and oil.

1.4.5 APPLICATION OF HYDROPHILIC AND UNDERWATER OLEOPHOBIC MATERIALS IN OIL-WATER SEPARATION WITH WATER-REMOVING METHOD

As mentioned above, it is difficult to manufacture hydrophilic and oleophobic materials. Inspired by fish scales, many hydrophilic and underwater oleophobic materials have been prepared for oil-water separation. [79-88] Theoretically, a surface that is superhydrophilic in air will exhibit superoleophobicity underwater. This is because the superhydrophilic surface traps water molecules onto its

layered surface structure to reach a low-energy state. When in contact with oil, the material exhibits superoleophobicity underwater because oil is energetically unfavorable to displace water molecules.

1.5 HONEYCOMB FILMS FABRICATED WITH BREATH FIGURE METHOD

1.5.1 INTRODUCTION OF BREATH FIGURE

Breath figure method is also a technology that people learn from nature and can be used to fabricate uniform porous films (honeycomb films). [89] Breath figure refers to the fog that forms when water vapor contacts a cold surface. We often see this phenomenon in our daily life, such as when we breathe on the window, the fog will appear on the window. This is the reason why the name "breath figure" comes from.

In 1994, François et al. found a method for manufacturing a honeycomb porous membrane by exposing a drop of polystyrene-b-polyparaphenylen (PS-b-PPP) solution in carbon disulfide (CS_2) to a flow of moist air. The polymer membrane with a microstructure fabricated in a bottom-up manner. [89] Over the past two decades, this simple process has been widely used as a general soft-template method to fabricate honeycomb-patterned films with controllable pore size and different potential functions and applications. [89-99]

Many researchers have reported that polymers with amphiphilic molecular structures are more likely to form ordered honeycomb films. If the polymer is not amphiphilic, the water droplets can be stabilized by adding a small number of amphiphilic molecules into the solution.

Shimomura et al. demonstrated that, with the aid of the surfactant CAP (copolymer of dodecylacrylamide and carboxyhexylacrylamide shown in Figure 1-11) ordered honeycomb films could be prepared from most liposoluble polymer solutions. [96,97]

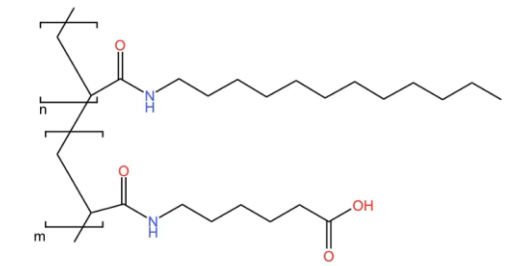

copolymer of amphiphilic polyacrylamide
CAP

Figure 1-11. Chemical structure of polymer CAP.

Conventional methods for micro-structure fabrication are irrelevant for fabrication on intricate and non-flat surfaces such as the inner surfaces of tubes and have the disadvantages of being energy-consuming and expensive.

The breath figure method has been an area of extensive research because it enables the fabrication of highly ordered honeycomb structures by self-organization on the sub-microscale and microscale.

1.5.2 BREATH FIGURE METHOD COMPARED WITH PHOTOLITHOGRAPHY

There are many ways to make porous materials, but most of them do not have uniform pore size. [100-105] Commonly used methods to prepare uniform pore size are photolithography, [106-110] the Langmuir–Blodgett technique [111-113] and breath figure method. [96,97]

Photolithography can create patterns down to tens of nanometers and enable precise control over feature geometry. But photolithography has many steps compared to the breath figure method, and the upfront investment is costly.

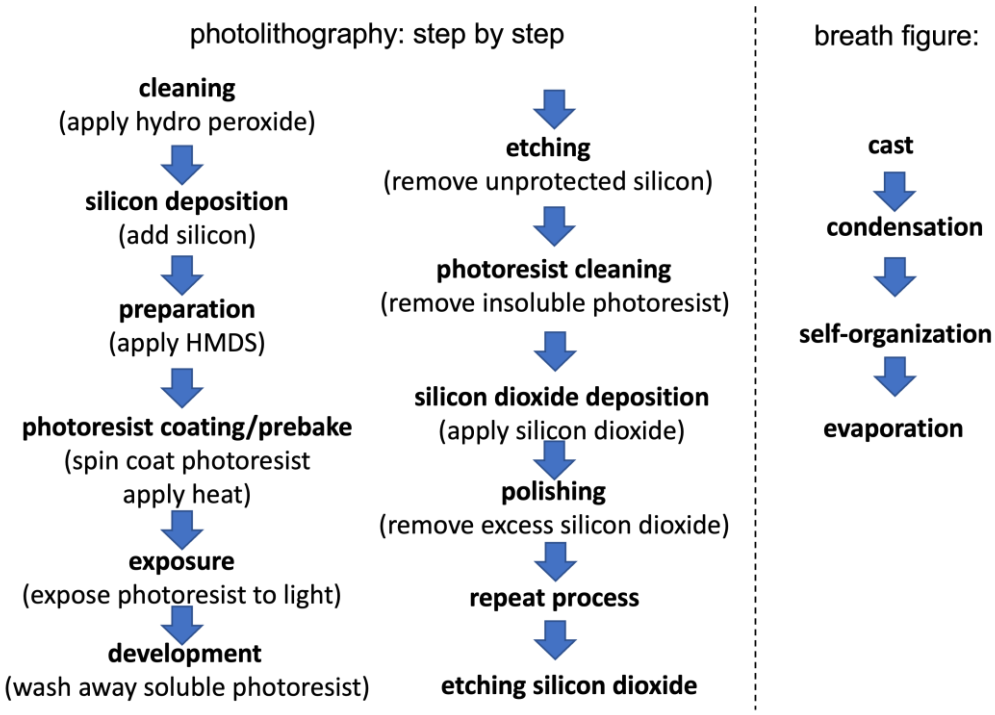

Figure 1-12. Steps of photolithography compared to the breath figure method.

And the Langmuir–Blodgett technique with a polystyrene template can also fabricate honeycomb structure films. One advantage of this method is that some materials that cannot be prepared by the breath figure method can be prepared. However, for materials that can be prepared by both methods, the breathing method is more energy-efficient, and the controllable range of uniform pore size is larger.

1.6 OBJECTIVES

Porous membranes cannot remove the small oil droplets from the oil-water mixture or the oil-in-water emulsions. Reducing the pore size usually accompanied by the significant increasing of the thickness because of the nonuniform pore size and then reduced the separation efficiency.

The honeycomb (HC) films have uniform pore size with several microns, interconnected structure and thickness about several microns. Most surface modifications to honeycomb films are for the single-side open structure honeycomb films. There are reports of using hydrophilic groups to modify the perforated honeycomb membrane, but theoretically it is not superhydrophilic after modification. The hydrophilicity of single-side open honeycomb films will increase with the UV-O_3 treatment time increasing.

In this thesis, I try to apply lubricated HC films after UV-O_3 treatment for liquid water-oil/emulsion separation membranes for the first time. Then, the new droplets generation from the HC film was observed for the first time and discussed the mechanism and origin of the phenomena in the thesis. The changes in the underwater transparency of HC films were discussed, which facilitates the macroscopic observation of different structures. The wettability changes of the same material under flat and honeycomb structures exceed previous theoretical values. Additionally, the penetration conditions of water, two kinds of oils, and emulsion into HC films were discussed in this thesis.

Therefore, this thesis is the first success of the UV-O_3 treated lubricated Honeycomb (HC) Films for sufficient oil-water separation membranes with gravity-driven system and also proposed novel insight of the phenomena and mechanism.

CHAPTER 2. PREPARATION OF HONEYCOMB FILMS

In this thesis, honeycomb films prepared by adding surfactant CAP into liposoluble polymer solutions.

2.1 FORMATION MECHANISM FOR HONEYCOMB FILMS

Conventional methods for micro-structure fabrication are irrelevant for fabrication on intricate and non-flat surfaces such as the inner surfaces of tubes and have the disadvantages of being energy-consuming and expensive.

The breath figure method has been an area of extensive research because it enables the fabrication of highly ordered honeycomb structures by self-organization on the submicroscale and microscale.

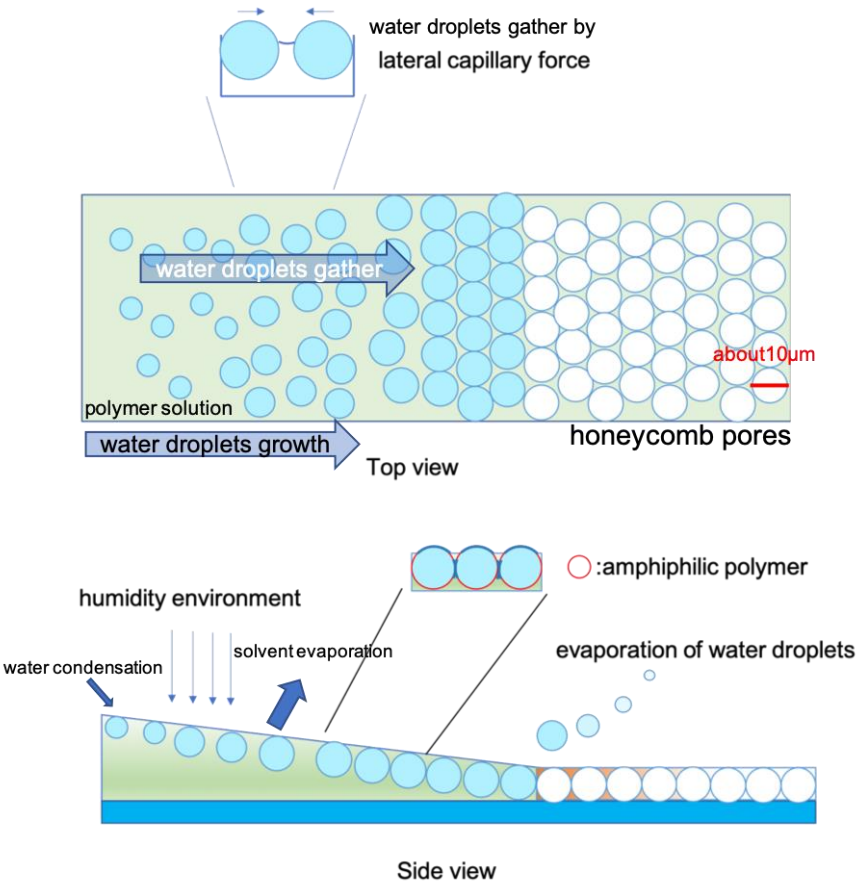

Figure 2-1. Schematic illustration of honeycomb-patterned film preparation.

When a mixed solution of a hydrophobic polymer and an amphiphilic polymer is cast on the substrate surface, the temperature of the solution surface decreases due to the heat of vaporization when the solvent volatilizes, and water droplets are condensed on the surface. Under the stable humidity environment, the water droplets become larger and larger. And condensed water droplets gather due to the lateral capillary force between the water droplets. The assembled water droplets are prevented from fusing together by the action of the amphiphilic polymer contained in the mixed solution. As a result, the water droplets are densely arranged, and the organic solvent is completely volatilized. Finally, a polymer film having regular pores where before were densely arranged water droplets is obtained after the water droplets evaporated.

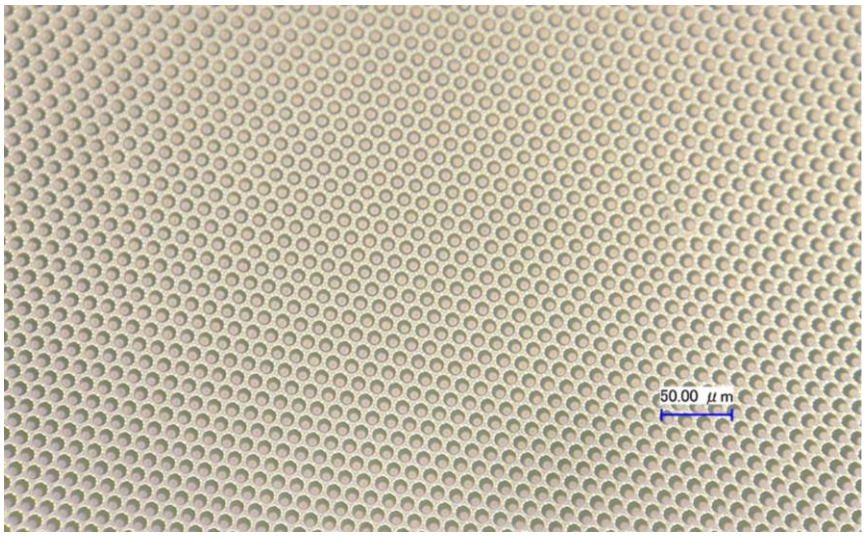

Figure 2-2. The optical microscope image of a honeycomb film.

In this chapter, the formation mechanism for honeycomb films will be discussed in three parts: water droplets condensation, growth and self-organized of water droplets and the evaporation of solvent and water droplets. It should be noted here that the formation of BFAs is a very complicated process, and no general mechanisms have adequately explained all experimental results.

2.1.1 WATER DROPLETS CONDENSATION

Cold surfaces are essential for water droplets to condense. When the surface temperature is below the dew point of the atmosphere, water vapor can spontaneously condense on the surface.

In this thesis, there are two methods to get a cold surface: (1) evaporative cooling method and (2) using a cold stage to directly cool the substrate and solution.

2.1.1.1 EVAPORATIVE COOLING METHOD

Although the use of a cold stage to directly cool the substrate and solution is an obvious method, honeycomb films can still be produced by relying solely on evaporative cooling.

Evaporative cooling means that when a solution with a high solvent evaporation rate is cast onto a substrate, the solvent begins to evaporate immediately, and the temperature of the solvent decreases rapidly due to the enthalpy of evaporation. During evaporation, the temperature of the chloroform solution drops to 0–6 °C,[114] significantly below the dew point of the atmosphere, so water vapor can condense on the surface of the solution.

Therefore, when using the breath figure method to prepare the honeycomb film, even if the substrate is not cooled in the preparation stage, when the solution containing chloroform is cast on a solid surface, the water droplets can condense on the surface of the polymer solution due to evaporative cooling.

2.1.1.2 COOLING SUBSTRATE METHOD

Using a cold stage to cool the substrate and solution directly is a convenient method when large-area thin films must be fabricated or when pore size needs to be controlled.

It is important to note that the substrate plays a crucial role in the water condensation process. The heat exchange between the solution and the substrate affects the temperature of the solution.

2.1.1.3 CRITICAL RADIUS FOR NUCLEATION

The nucleation of water vapor is the first step in the formation of an array of water droplets.

Condensation of vapor is a nucleation process similar to boiling of liquid. [115-116] When the vapor temperature is below the saturation temperature corresponding to its pressure, the vapor is in a supersaturated metastable state. Metastable supersaturated vapor is a homogeneous system macroscopically, and microscopically, due to the thermal motion and collision of molecules, not only the usual density fluctuations, but also the phenomenon that multiple molecules aggregate into liquid nuclei frequently occur. Of the many liquid nuclei formed instantaneously, only those larger than

$$R_c = \frac{2\Upsilon_{LG}V}{RT\ln(P/P_{eq})} \qquad (2-1)$$

where P is vapor pressure in the gas phase, P_{eq} is the bulk liquid equilibrium vapor pressure. When $\mathrm{T}=300\mathrm{K}$, $\Upsilon_{LG} = 72mN/m$, $\mathrm{P}=1.1\mathrm{P_{eq}}$, $R_c=100\mathrm{nm}$.

Thus, the polymers in the solutions can influence the nucleation because they determine the surface tension of the solution. If the surface tension of the solution is sufficiently low (or the solution is very hydrophobic), the nucleation will be suppressed.

So, for water droplets that condense on the polymer solution surface, the initial radius is the same.

2.1.2 GROWTH AND SELF-ORGANIZED OF WATER DROPLETS

The main feature of the honeycomb film is the hexagonal close-packed pores, which indicate the existence of an ordered array of water droplets on the surface of the uncured polymer solution. To elucidate the formation mechanism of the honeycomb film, the growth of water droplets and the formation of the hexagonal droplet lattice must be explained. In this section, the growth and self-assembly of water droplets and how to control the pore size will be discussed.

2.1.2.1 GROWTH OF THE WATER DROPLETS

Pore size is an important parameter for honeycomb membranes, as many applications depend on the average pore size. The condensation nucleation of water at the surface has been discussed earlier. After nucleation, if we assume that the temperature remains constant throughout the growth. In this case, the growth rate of the droplet volume (V) is proportional to the concentration gradient in the boundary layer, the mass diffusivity, and the saturation pressure difference [117]

$$\frac{dV}{dt} \sim D\Delta p C_0 \delta^{-1} \qquad (2-2)$$

where D is the diffusion coefficient of water molecules in the carrier gas, Δp is the saturation pressure difference of water between the environment and the surface of the substrate, C_0 is the concentration of water in the carrier gas, and δ is the length scale of the condensation gradient, which is related to viscosity, the velocity of the gas flow, and D. Near room temperature, the growth of water droplets is described as

$$R \sim (D\Delta p C_0 \delta^{-1} t)^{1/3} \qquad (2-3)$$

From equation 2-3, when the growth time is increased, the average radius of the water droplets will increase.

In my thesis, when I control the speed of the air blow, the concentrate of polymer, the cast volume of polymer solution and the moving speed of substrate

unchanged, with the temperature of the substrate decrease, the average radius of the water droplets will increase because the growth time is increased.

Table 2-1. Pore size and temperature of the substrate relationship with PB/CAP in $CHCl_3$.

T of substrate (℃)	pore size (μm)	cast V (mL)	Concentrate (g/L)	T of air blow (℃)
20	2~3	20	5	30
14	5	20	5	30
7	10	20	5	30
3	14	20	5	30

2.1.2.2 STABILITY OF WATER DROPLETS

When polymers with amphiphilic molecules are directly used as materials for preparing honeycomb films, most of the honeycomb films formed are non-interconnected. Adding amphiphilic polymers to hydrophobic polymers can make the honeycomb structure more uniform, easier to form in large areas and interconnected internally. [96.97,118-120]

As shown in Figure 2-3 [118], only the DOPE/PLA can form the uniform honeycomb structure. And the DLPC/PLA cannot even form irregular pore size because of the interfacial tension of the polymer solution–water is low. It is necessary to investigate the shape of the water droplets suspended on the surface of an organic solution because the shape of the water droplets determines the shape of the pores in the BFAs and is related to the self-assembly process. When a small volume of liquid is dropped onto the surface of another immiscible liquid, it may form a droplet or spread as a thin film.

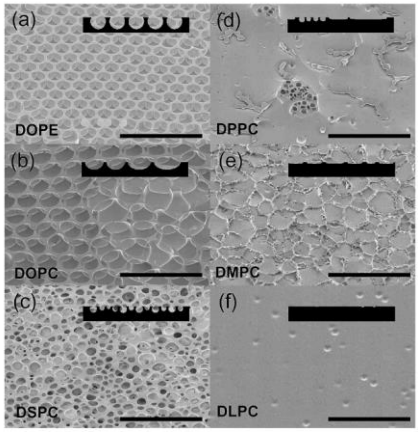

Figure 2-3. FE-SEM images of film surfaces. (a) PLA/DOPE, (b) PLA/DOPC, (c) PLA/DSPC, (d) PLA/DPPC, (e) PLA/DMPC, and (f) PLA/DLPC. The scale bar represents 20mm. Schematic views show the cross-sectional structure of each film. (Reproduced with permission, Copyright 2008, Royal Society of Chemistry) [118]

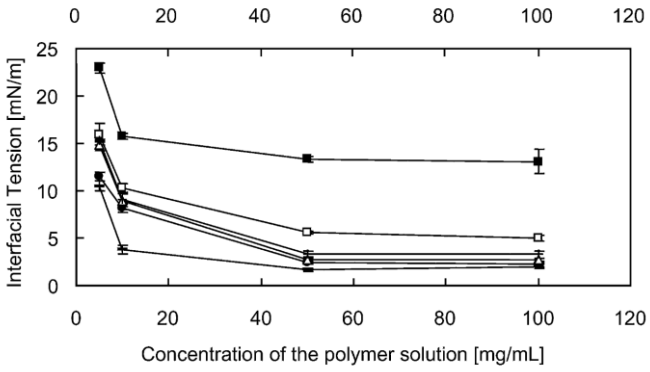

Figure 2-4. Interfacial tension of phospholipids at the polymer solution–water interface as a function of total polymer concentration. ■: DOPE, □: DOPC, +: DSPC, △: DPPC, ・: DMPC, —: DLPC. [118] (Reproduced with permission, (Reproduced with permission, Copyright 2008 Royal Society of Chemistry)

When studies a liquid spreading in another liquid, the spreading coefficient (S) could be written as follows,

$$S = \gamma_a - (\gamma_b + \gamma_{a/b}) \qquad (2-4)$$

where γ_a is the surface tension of the polymer solution, γ_b is the surface tension of the water droplet, and $\gamma_{a/b}$ is interfacial tension between the polymer solution and the water droplets in this case. This means that a water droplet with low surface tension cannot maintain a globular shape. As mentioned before, water droplets do not spread on the surface of organic solvents. However, for organic droplets, the situation is complicated because γ_a and γ_b are comparable. Small amounts of surfactant may severely alter spreading behavior. Small water droplets can remain spherical because the surface tension of water is relatively high. However, for other liquids, the droplet may deform from the sphere when pressed.

2.1.3 SOLVENT AND WATER EVAPORATION

And condensed water droplets gather due to the lateral capillary force between the water droplets. The action of the amphiphilic polymer contained in the mixed solution prevents the assembled water droplets from fusing together.

Many researchers have reported that polymers with amphiphilic molecular structures formed honeycomb structures much more easily. [87,96] But most of these kind of honeycomb films are not interconnected as shown in Figure 2-5. [121]

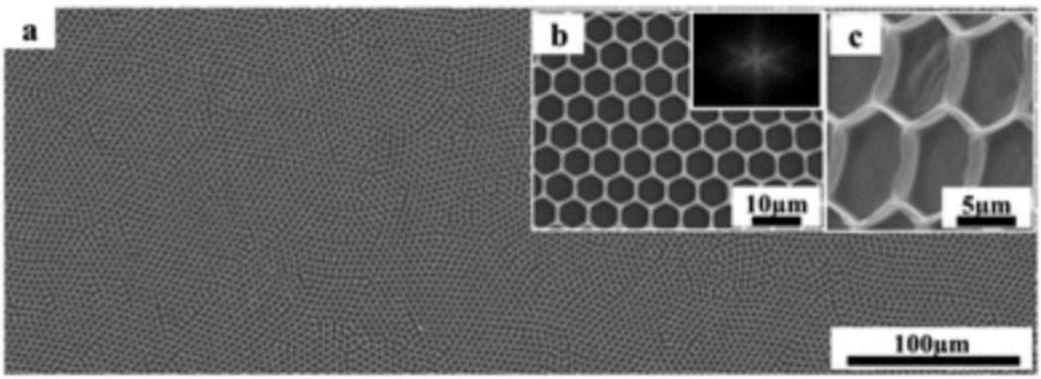

Figure 2-5 SEM images showing the shapes of pores in the polymer films prepared by breath figure method without amphiphilic polymer. [121]
(Reproduced with permission, Copyright 2014 Royal Society of Chemistry)

Amphiphilic molecules tend to assemble at the water/solution interface and form a protective layer. The amphiphilic-molecule-protected water droplets on the surface of a polymer solution comprise a two-dimensional emulsion that is quite stable. If the polymer is not amphiphilic, the water droplets can be stabilized by adding a small number of amphiphilic molecules into the solution. In this thesis, with the aid of the surfactant CAP, honeycomb structure could be prepared from most liposoluble polymer solutions with interconnected structure as shown in Figure 2-6.

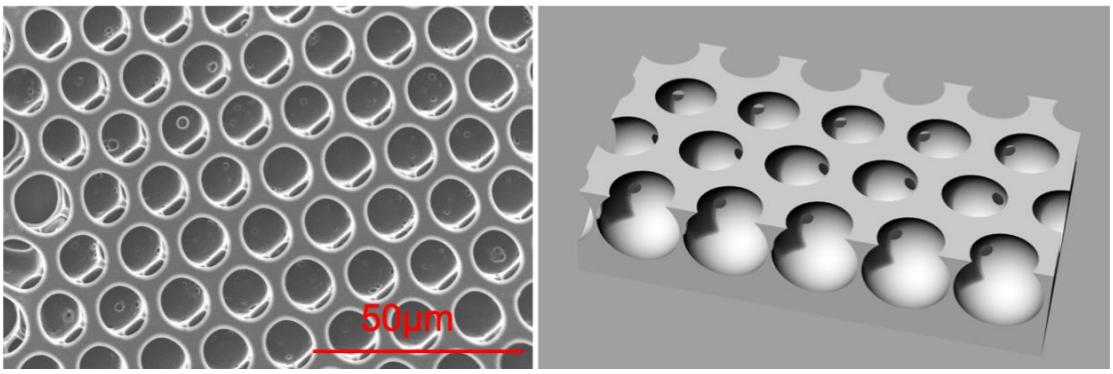

Figure 2-6. The SEM image and model of the interconnected honeycomb film.

2.2 MORPHOLOGICAL CONTROL OF HONEYCOMB FILMS

2.2.1 MATERIALS OF PREPARATION OF HONEYCOMB FILMS

As mentioned before, with the aid of the surfactant CAP ordered honeycomb films could be prepared from most liposoluble polymer solutions. [96,97]

In this thesis, with adding the amphiphilic polymer CAP, we can fabricate the honeycomb films with polystyrene, polysulfonate, poly(1,2-butadiene), poly(bisphenol-A-carbonate) and poly(ε-caprolactone). (Figure 2-7)

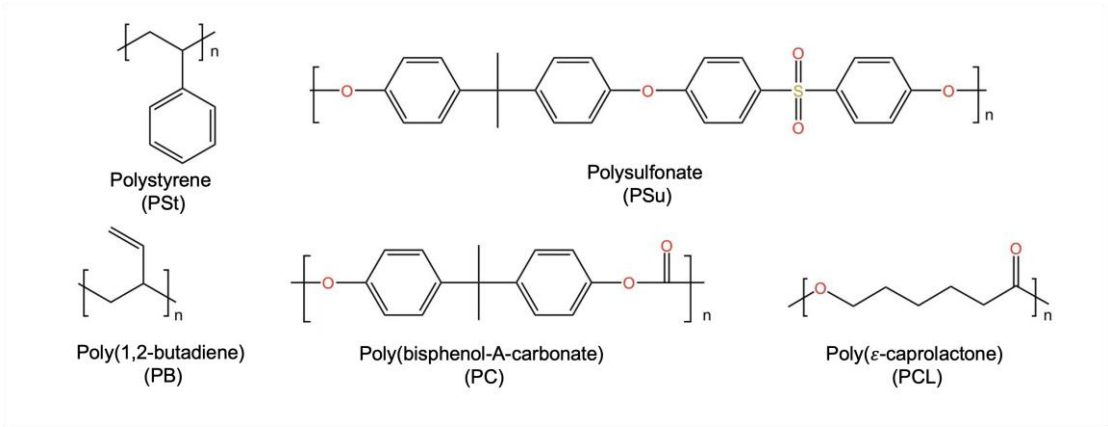

Figure 2-7. Various kinds of hydrophobic polymers.

2.2.2 SUBSTRATE OF PREPARATION OF HONEYCOMB FILMS

With adding the amphiphilic polymer CAP, we can fabricate the honeycomb films on flat PET, flat glass, Al, PET mesh and also in glass tube.

2.2.3 PINCUSHION-LIKE STRUCTURES OBTAINED FROM HONEYCOMB FILMS

After the honeycomb films was prepared by the breath figure method with adding CAP, the pincushion-like (PC) structures can also be obtained by simply peeling off the top layer of the honeycomb film using adhesive tape. (Figure 2-8)

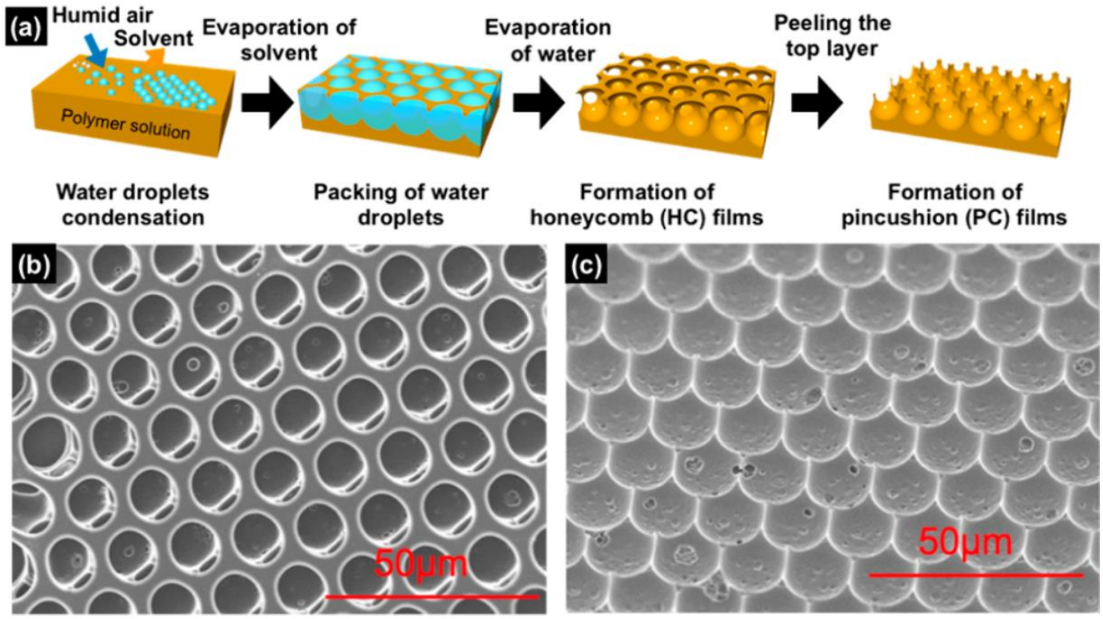

Figure 2-8 (a) Schematic illustration of pincushion film preparation. (b) SEM of the HC film. (c) SEM of the PC films. [86] (Reproduced with permission, Copyright © 2020, American Chemical Society)

SEM images clearly show that each pillar was broken at its center after peeling off the top layer using adhesive tape, and a highly ordered pincushion-like structure was obtained. We can see the column more intuitively by tilting the coating at a certain angle. (Fig 2-8)

2.2.4 PREPARATION OF PERFORATED HONEYCOMB FILMS

When fabricate the honeycomb film on hydrophilic glass (water contact angle in air near 90°), reduce the concentrate of polymer solution could shorten the distance between the water droplets and the glass. (Figure 2-9)

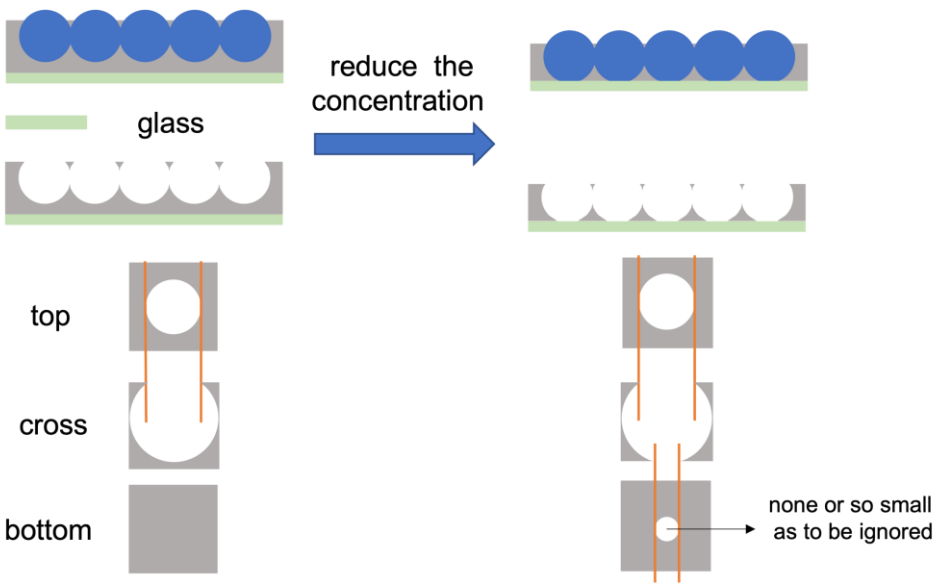

Figure 2-9. Schematic of the water droplets change with the polymer solution concentrate decreasing.

The experimental results show that even if the concentration is reduced, it is difficult to form the pore at the bottom. That is to say, the water contact angle on glass in polymer solution is very large.

The glass is hydrophilic, and if increasing the hydrophilicity of the glass, the surface tension of water and substrate will increase. So，by increasing the affinity of water to the substrate, the fabrication of the perforated honeycomb film is fabricated possible. (Figure 2-10)

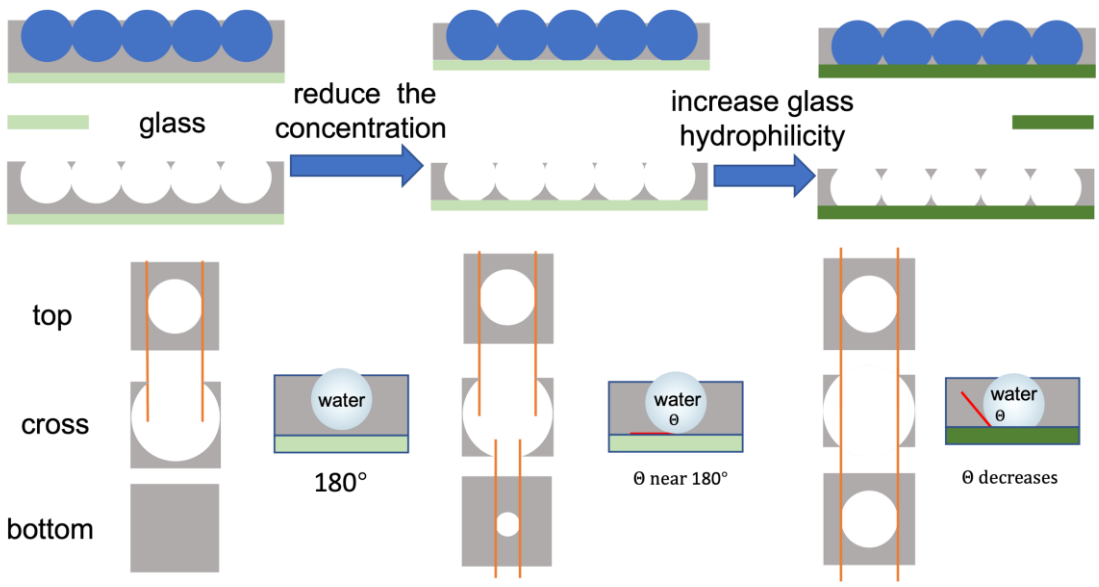

Figure 2-10. Schematic of the water droplets change with the decreasing concentration and increasing glass hydrophilicity.

Reduce the concentrate of the polymer solution and fabricate the honeycomb film on hydrophilic substrate (such as the glass treated with UV-O_3 for 15min), we can fabricate the perforated honeycomb films as shown in Figure 2-11. If using other hydrophilic materials as substrates, the perforated honeycomb films could also be fabricated.

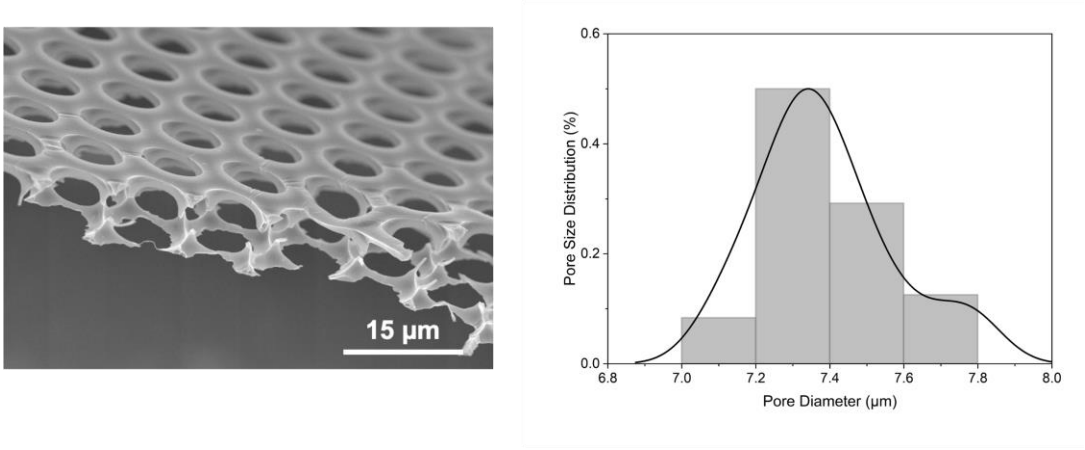

Figure 2-11. The SEM image and pore size distribution of the perforated honeycomb film.

2.2.5 CONTROLLABLE PORE SIZE OF HONEYCOMB FILMS

The pore size is determined by the water droplets. And as mentioned before, for water droplets that condense on the polymer solution surface, the initial radius is the same. We can control the substrate temperature to adjust the droplet growth time, and then control the pore size of honeycomb films.

Table 2-2. Pore size and temperature of the substrate relationship with PB/CAP in $CHCl_3$.

T of substrate (℃)	pore size (μm)	cast V (mL)	Concentrate (g/L)	T of air blow (℃)
20	2~3	20	5	30
14	5	20	5	30
7	10	20	5	30
3	14	20	5	30

When other conditions are the same, the higher the substrate temperature, the smaller pore size of honeycomb films (Table 2-2).

2.2.6 CHEMICAL MODIFICATION OF HONEYCOMB FILMS

With the UV-O_3 treatment, the hydrophilicity the polystyrene honeycomb films and polybutadiene honeycomb films could increase. [122,123]

From X-ray photoelectron spectroscopy (XPS) reported in the previous report, -C=O, -COOH, and C-OH moieties formed after UV–O_3 treatment as shown in Figure 2-12. [122]

After UV-O_3 treatment, a hydrophilic film can be obtained, and the original honeycomb structure or pincushion structure is still maintained.

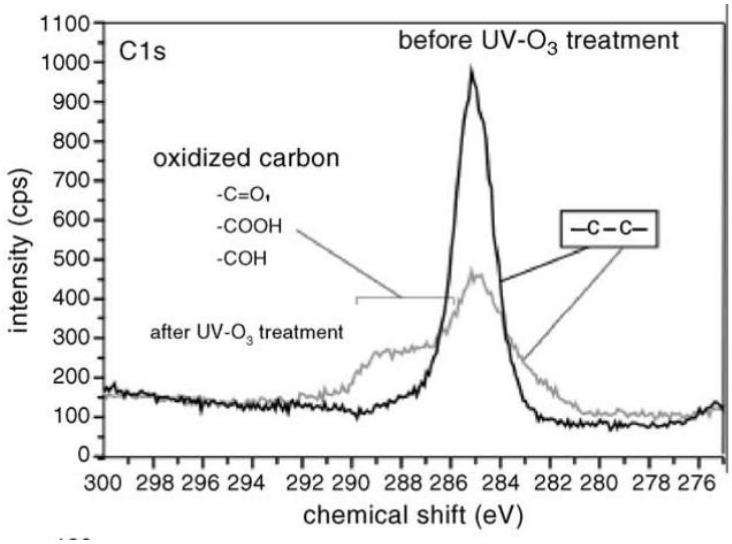

Figure 2-12. XPS spectra of the polystyrene honeycomb-patterned film before and after exposure of UV-O_3. [122] (Reproduced with permission, Copyright © 2005 Elsevier B.V. All rights reserved.)

2.3 UNDERWATER OLEOPHOBIC AND TRANSPARENT HONEYCOMB FILMS

The hydrophobic and oleophilic honeycomb films can be fabricated and expected to be used in oil-water separation. At the same time, UV-O_3 treatment can obtain hydrophilic honeycomb films. Whether this honeycomb membrane has the property of underwater oleophobicity like fish scales is a very critical question.

Recently, there has been growing interest in the design of underwater superoleophobic surfaces as they are of great importance in academia and industry, including topics such as underwater antifouling, oil-water separation, bio-adhesion, and minor oil droplet manipulation. [124-128] In nature, water can become trapped in the rough microstructure of fish scales, creating an oil-repellent lubricating layer. The water lubricating layer brings underwater oleophobicity and ultra-low oil adhesion, giving the fish scale oil resistance underwater. Inspired by fish scales, a variety of underwater superoleophobic surfaces were artificially fabricated.

At the same time, the change of the transparency of the porous film in air and underwater has also attracted attention for underwater transparent films can be used in oil-repellent lenses for underwater cameras, diving goggles, and imageable substrates.

In nature, there is a fantastic phenomenon in which the petals of Diphylleia grayi will turn from white to transparent in the rain, as shown in Figure 3-12. [124]

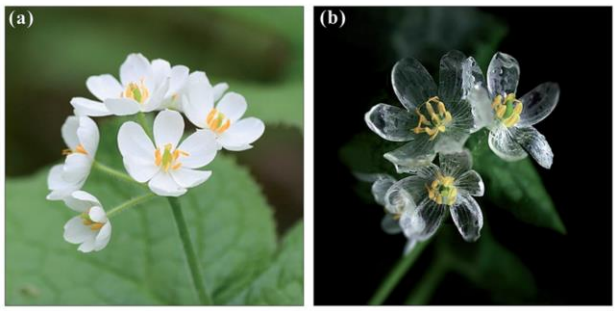

Figure 2-13. (a)The white petals on a sunny day and (b) transparent in the rain. [124] (Reproduced with permission, Copyright 2015 Royal Society of Chemistry)

The process of increasing transparency is the process of the liquid gradually replacing the air, and also the process of changing from Cassie mode to Wenzel mode.

The polybutadiene honeycomb films with the pore size of 5μm, 7μm and 9μm which were labeled as 5HC0, 7HC0 and 9HC0, respectively. And the contact angle and transmittance of HC films with different pore sizes were shown in Figure 2-14. As the pore size decreases, the contact angle gradually increases, but this change is very small. In air, as the pore size of the honeycomb membrane increases, the transparency increases slightly. But overall, the transparency of honeycomb films with different pore sizes is very low. The difference in contact angle of honeycomb films with different pore sizes (5μm, 7μm and 9μm) is very small, and the difference in transparency is also very small. Therefore, in the subsequent experiments, only the honeycomb films with a pore size of 5 μm was treated and measured.

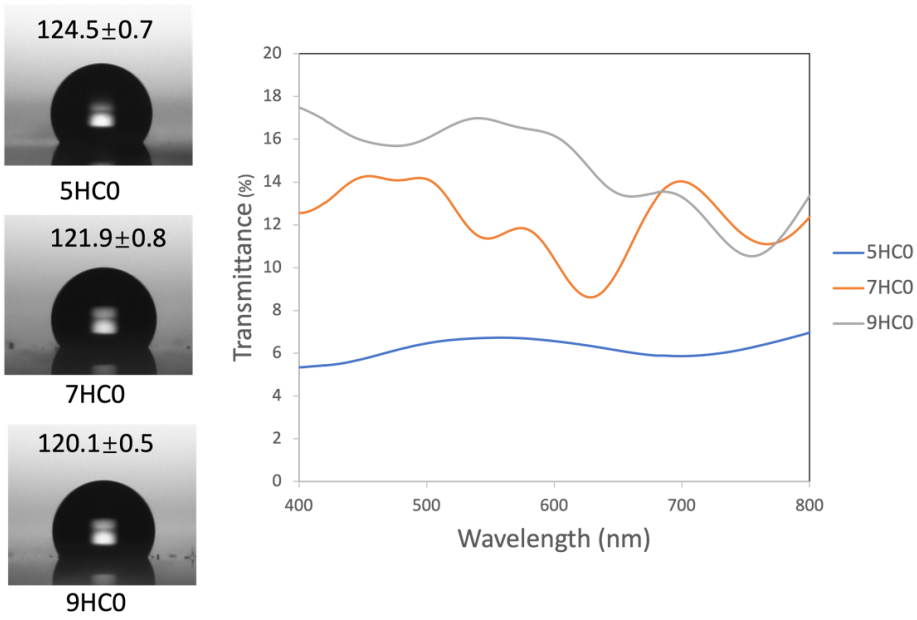

Figure 2-14. Contact angle and transmittance of 5HC0, 7HC0 and 9HC0.

The transmittance of different HC films is poor. Chose the HC films with 5μm diameter and treated the 5HC0 with UV-O_3 for 60 min and labeled as 5HC60.

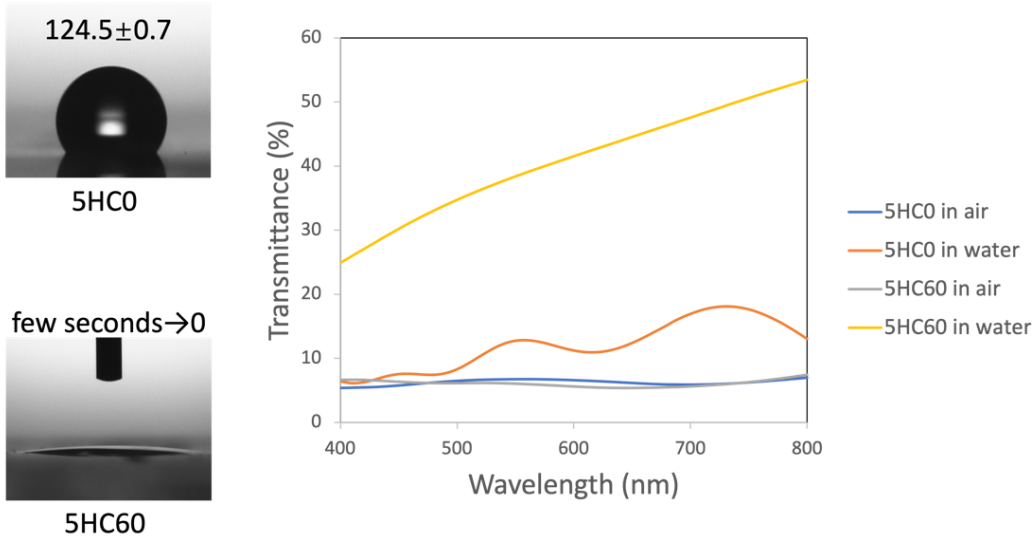

Figure 2-15. Contact angle in air and transmittance of 5HC0 and 5HC60 in air and water.

The HC films after 60 min UV-O_3 treatment has change to superhydrophilic with the water contact angle is 0°. But the transparency of 5HC0 and 5HC60 in air

did not change. This shows from another perspective that after 60 min of UV-O_3 treatment, the structure of the honeycomb film has not changed. At the same time, it also shows that the hydrophilization treatment does not affect the transparency. When the transparency changes in the experiment, the influence of the change of the material itself can be ignored.

And the transparency of 5HC60 in water has improved. This transparency changing from the 5HC0 to 5HC60 is also the water state changing from Cassie mode to Wenzel mode. The hydrophilic honeycomb can trap the water in the porous structure like fish scales.

The pincushion (PC) structure films after peeling off the top layer of 5HC60 and labeled as 5PC60.

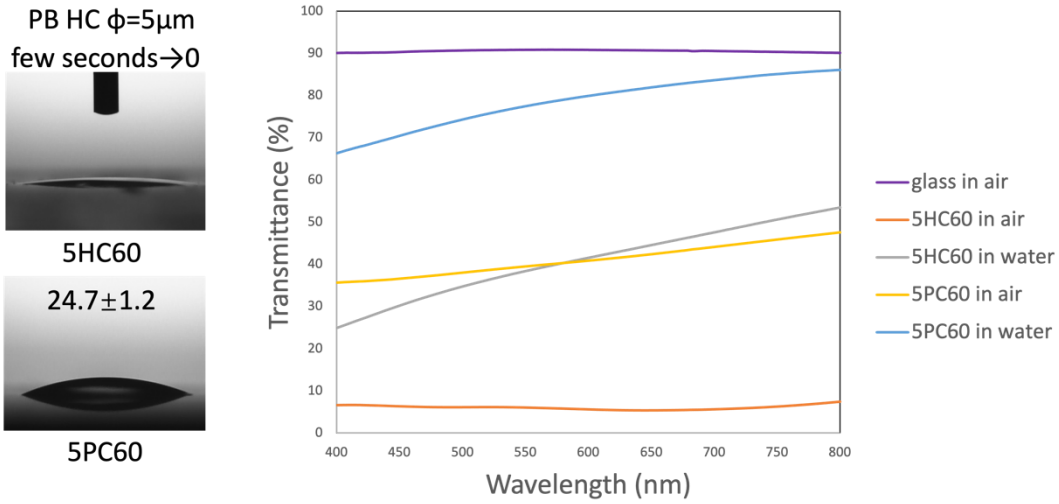

Figure 2-16. Contact angle in air and transmittance of 5HC60 and 5PC60 in air and water.

The transparency of 5PC60 in water has significantly improved. The superhydrophilic pincushion film change to superoleophobic underwater and at the same time become transparent as shown in Figure 2-17.

Figure 2-17. Oil droplet on the 5PC60 underwater and the image on a piece of paper.

An underwater transparent and superoleophobic film has been successfully prepared and is expected to be used in underwater cameras, diving goggles and oil-resistant lenses for imaging substrates. And the wettability change from superoleophilic in air to superoleophobic underwater is important for oil water separation.

2.4 BUBBLE GENERATION FROM HONEYCOMB FILMS

When measuring the oil contact angle underwater, droplets are generated from the honeycomb film when the oil droplet contact the surface of the honeycomb film. (Figure 2-18)

By comparing the two pictures, we can see that the volume of the oil droplet has become smaller, and a lot of unknown droplets have appeared. The contact angle of decane is very large, about 154.3°. And the contact angle of unknown droplets is very large too. The size of the droplets generated from the honeycomb film varies, and there is no regularity. The first unknown droplet that appears, after stabilization, is not the biggest one.

In order to know if this phenomenon is an accidental phenomenon, repeat the experiment and record.

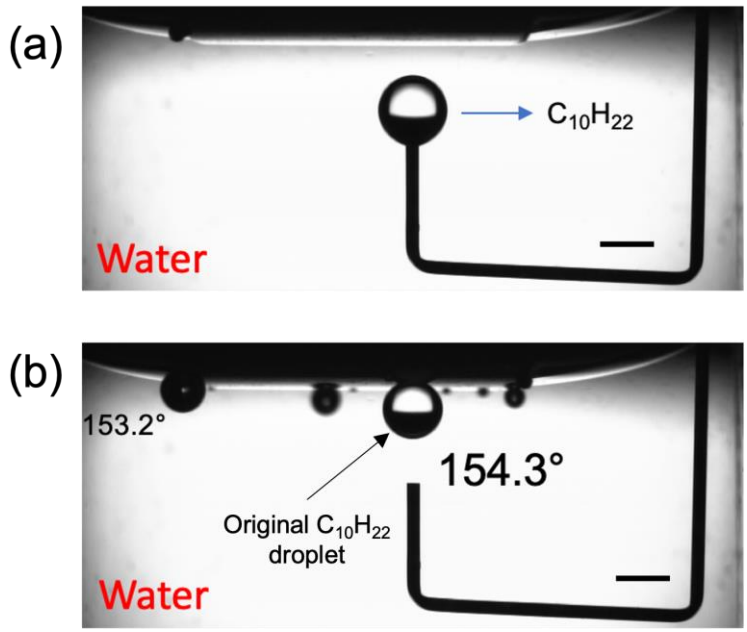

Figure 2-18. The image of the phenomenon and contact angle. (bar =1 mm)

The polybutadiene honeycomb films treated with the UV-O_3 for 0 min,30 min and 60 min which were labeled as HC0, HC30 and HC60, respectively. The pincushion (PC) structure films after peeling off the top layer of HC30 and HC60 were labeled as PC30 and PC60, respectively.

Table 2-3. The contact angle on samples. Θ_{wa}: water CA in air, Θ_{oa}: oil (decane) CA in air, Θ_{ow}: oil (decane) CA in water. "Absorbed" means the oil droplet is absorbed and other droplets appear.

sample	Θ_{wa} (°)	Θ_{oa} (°)	Θ_{ow} (°)
HC 0	123.1	0	Absorbed (125.0)
HC 30	106.5	0	Absorbed (154.3)
HC 60	0	0	161.0
PC 30	79.4	0	167.7
PC 60	37.2	0	160.1

With the time of UV-O_3 increasing, the water contact angle decreases whether on HC film or PC film.

Although the hydrophilic treatment makes the water contact angle decrease, the oil contact angle does not change, and is always 0°. This is consistent with the previously mentioned relationship between surface tension and wettability。

There is an abnormal phenomenon during the decane contact angle measurements on HC0 and HC30. These films show high decane contact angle, but the volume of the decane droplet decreases when it is attached to the surface. Furthermore, a lot of droplets have appeared from the surface of the HC film after attaching the decane droplet.

There is no droplet generated from HC60, PC30 and PC60.

Repeat the experiment and the same phenomenon occurs. And the process with the oil droplet absorbed and droplets generated from the surface was photographed at different times. (Figure 2-19)

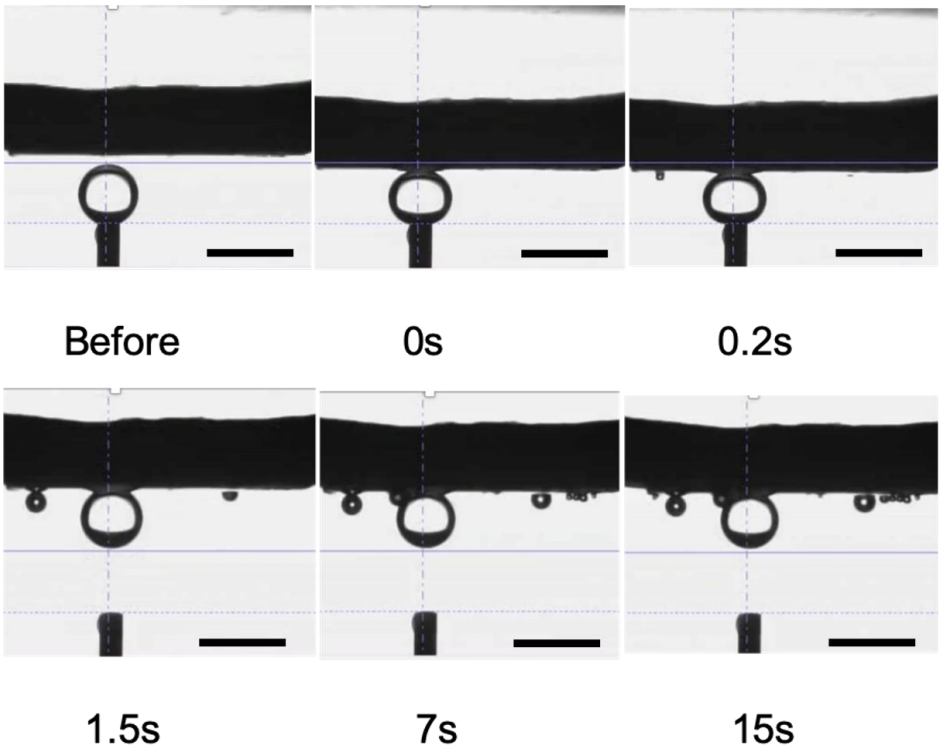

Figure 2-19. Process of the decane droplet contact with the PB honeycomb film. (bar=1 mm)

We can see that when the decane droplet contacts with the hydrophobic PB honeycomb film, the oil droplet is sucked into the film and then some droplets come out from the film. The droplets coming out from the film gradually become larger as the oil droplets decrease. Finally, the size of the oil droplet and the unknown droplets stop changing. The experiment showed more droplets, and a lot of very small droplets appeared (Figure 2-19).

In order to solve the question, a dyed red decane droplet ($3\mu L$) was released from beneath the substrate using a syringe. (Figure 2-20)

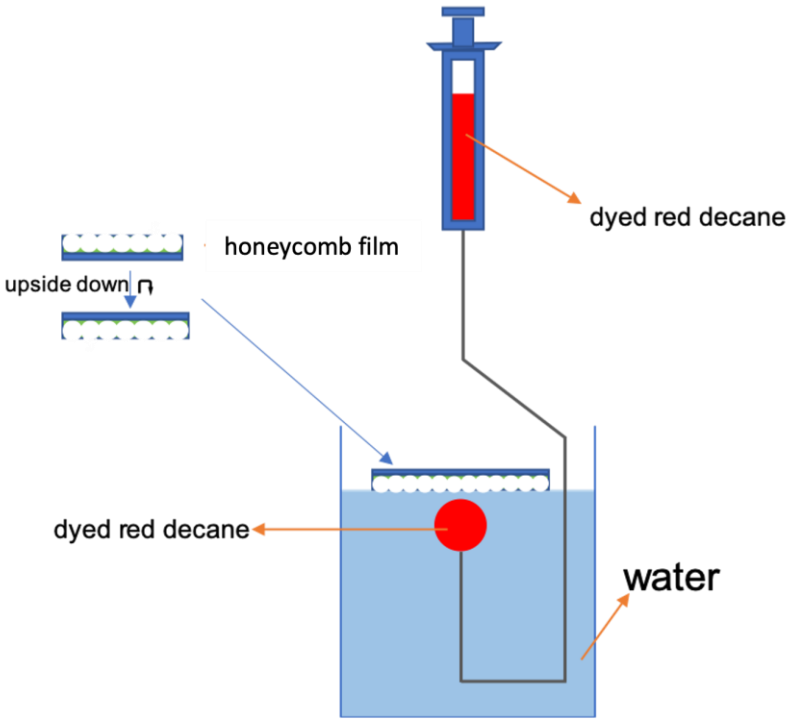

Figure 2-20. Schematic description of measurement of contact angles by the captive red decane droplet method for underwater conditions

After the droplets are stabilized, observe and take pictures with an optical microscope (BX51, Olympus). (Figure 2-21) We can clearly see that the oil droplet is red and the droplets running out of the film is transparent, so what come out from the film are not oil droplets. So, they are air bubbles. (Figure 2-22)

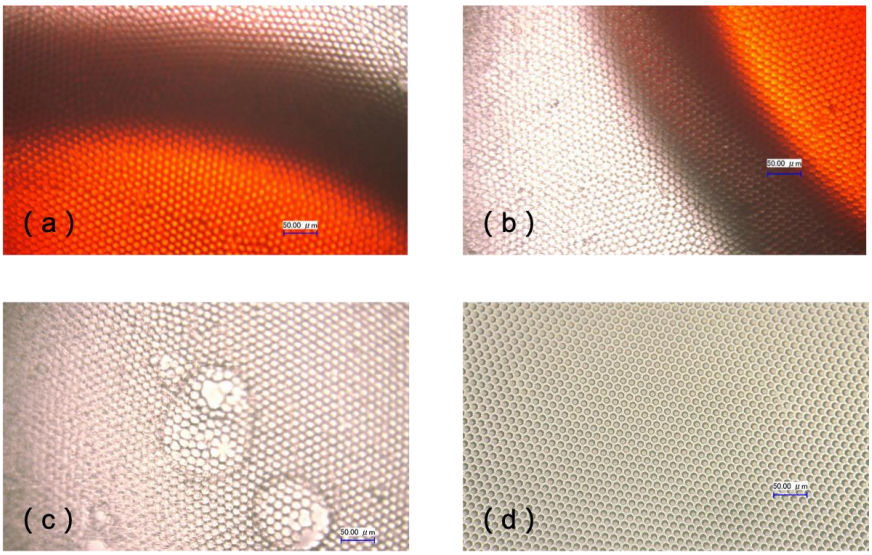

Figure 2-21. Images (a) and (b) show the red droplet on the HC 30. Images (c) shows transparent droplets on the HC 30. Images (d) shows the HC 30 in the air as a comparison. (bar=50μm)

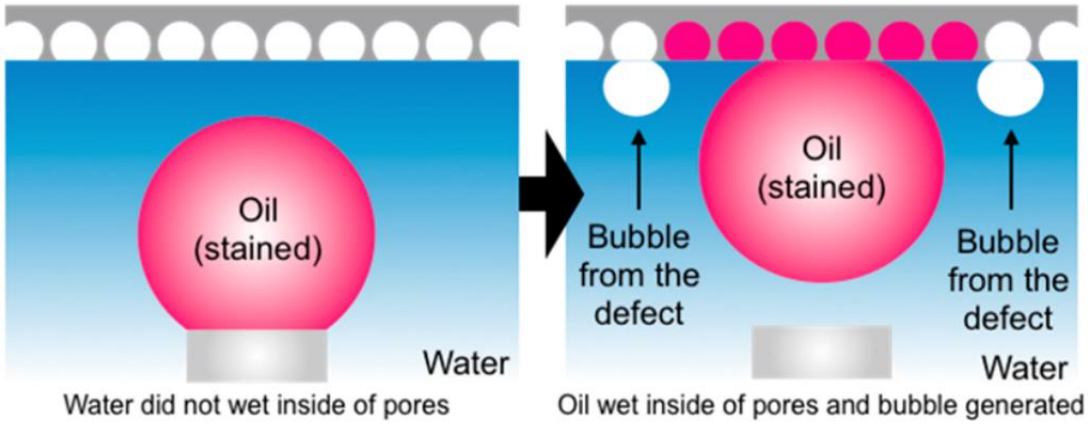

Figure 2-22. Underwater bubble and oil repellency on honeycomb and pincushion films with Cassie and Plastron state

Figure 2-21 shows that red-colored decane spread into the honeycomb pores and pushed air inside the honeycomb structure. And then, air bubbles are generated from the defects on the surface of the honeycomb structures. The air goes into the gas phase inside the honeycomb films, but air cannot be leaked from the surface of uniform-sized pores of honeycomb films due to the water pressure. However, bubbles are generated from the defected part of the honeycomb films since the large aperture of the defect breaks the balance

between air pressure and water pressure. Then the air bubble finally leaked from the defect site, as shown in Figure 2-22. This kind of air chamber system has been observed in the insect living underwater and is known as “plastron”. [129] To increase gas exchanging efficiency at the gill, and some insects keep the air by using their hydrophobic hairs as a gas chamber.[130] The hydrophobic honeycomb film works as a gas chamber underwater. Thus, this system is one of a good example of biomimetic materials. [131]

Although the oil contact angle is still large on the hydrophobic honeycomb film, the oil droplet can be absorbed in the honeycomb structure. Therefore, the hydrophobic surface underwater is still oleophobic and I marked the underwater contact angle of the oil as 0 with the hydrophobic honeycomb films that can absorb oil droplets underwater.

The liquid on solid surface in air spread coefficient S can be defined as

$$S = -(\Upsilon_{SL} + \Upsilon_{LG} - \Upsilon_{SG}) \qquad (2-5)$$

so, the oil droplet on the PB flat film underwater spread coefficient S_{flat} can be defined as

$$S_{flat} = -\left(\Upsilon_{SO-flat} + \Upsilon_{OW} - \Upsilon_{SW-falt}\right) \qquad (2-6)$$

where Υ_{SO} is the surface tension of oil and the PB flat film, Υ_{OW} is the surface tension of oil and water, Υ_{SW} is the surface tension of the PB flat film and water.

In Wenzel model, a hydrophobic surface with Θ>90°, increasing the roughness of the material can make the surface more hydrophobic, and for a hydrophilic surface with Θ<90°, increasing the roughness of the material makes the surface more hydrophilic. When the oil droplet on the solid surface, an oleophobic surface with Θ>90°, increasing the roughness of the material can make the surface more oleophobic, and for an oleophilic surface with Θ<90°, increasing the roughness of the material makes the surface more oleophilic.

Table2-4. The contact angle on samples. Θ_{wa}: water CA in air, Θ_{oa}: oil (decane) CA in air, Θ_{wo}: water CA in oil (decane).

	UV-O_3 [min.]	Θ_{wa} [°]	Θ_{oa} [°]	Θ_{wo} [°]
PB	0	123.0	16.9	169.3
PB15	15	116.8	34.4	150.1
PB30	30	106.0	~0	126.9
PB45	45	~0	~0	112.8

For honeycomb films, as the hydrophilicity of the solid surface increases, the surface tension of the solid surface increases and the water contact angle in oil decreases. Therefore, the increase of solid surface tension will increase the spreading coefficient of water on the solid surface in oil. It is same for flat surfaces: increasing the hydrophilicity of flat solid will increase the surface tension of the flat solid. And the spreading coefficient of water on the flat glass in oil increased. This is also why the water contact angle on the flat glass in $CHCl_3$ decreases after the glass is hydrophilized when preparing the perforated honeycomb films. Due to the rough structure of the honeycomb membrane surface, the surface tension is smaller than that of the flat surface. That is to say, the surface tension of the PB flat film is greater than that of the honeycomb membrane, so the spreading coefficient of the water droplet is also larger than that of the PB honeycomb film.

$$\therefore S_{flat} - S_{HC} => 0 \qquad (2-7)$$

The equation (2-6) can be transfer to

$$S_{flat} = -\Upsilon_{OW} - \left(\Upsilon_{SO-flat} - \Upsilon_{SW-falt}\right) \qquad (2-8)$$

It can be obtained from Young's equation

$$\Upsilon_{SO-flat} = \Upsilon_{SG-flat} - \Upsilon_{OG-flat}\cos\Theta_{oa-flat} \qquad (2-9)$$

$$\Upsilon_{Sw-flat} = \Upsilon_{SG-flat} - \Upsilon_{WG-flat}\cos\Theta_{wa-flat} \qquad (2-10)$$

where $\Theta_{oa-flat}$ is the oil contact angle on PB flat film in air, $\Theta_{wa-flat}$ is the water contact angle on PB flat film in air, $\Upsilon_{SW-flat}$ is the surface tension between water and PB flat film in air, $\Upsilon_{SO-flat}$ is the surface tension between oil and PB flat film in air.

So,

$$\left(\Upsilon_{SO-flat} - \Upsilon_{SW-falt}\right) = -\Upsilon_{OG-flat}\cos\Theta_{oa-flat} + \Upsilon_{WG-flat}\cos\Theta_{wa-flat} \quad (2-11)$$

$$S_{flat} = -\Upsilon_{OW} + \Upsilon_{OG-flat}\cos\Theta_{oa-flat} - \Upsilon_{WG-flat}\cos\Theta_{wa-flat} \quad (2-12)$$

In the experiment, the oil is decane, $\Upsilon_{OW} = 50\ mN/m$, $\Upsilon_{OG-flat} = 24mN/m$, $\Upsilon_{WG-flat} = 72.8\ mN/m, \Theta_{wa-flat} = 93.0°$.

$$S_{flat} = -50 + 24\cos\Theta_{oa-flat} - 72.8 \times 0.05 = -53.8 + 24\cos\Theta_{oa-flat}$$

$$\because 24\cos\Theta_{oa-flat} < 24$$

$$\therefore S_{flat} < -53.8 + 24 < 0$$

$$\therefore S_{HC} < S_{flat} < 0 \quad (2-13)$$

So, the oil droplet cannot spread on the honeycomb film underwater.

The Laplace equation mentioned before is

$$\Delta P = \frac{2\Upsilon}{R} \quad (2-14)$$

where Υ is the surface tension, R is the principal radii of curvature.

For the oil Laplace pressure on the honeycomb film,

$$\Delta P = -\frac{2\Upsilon_{OG}\cos\Theta_{oa}}{d} \quad (2-15)$$

where d is the diameter of the pore size of the honeycomb film.

And the schematic of the Laplace pressure of the oil on the honeycomb film shows in Figure 2-15.

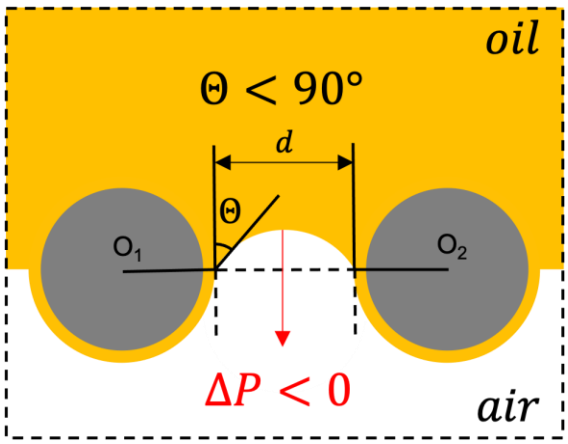

Figure 2-15. The schematic of the oil Laplace pressure.

And in the vertical direction of the oil droplet, the Laplace pressure on it is a vertical upward pressure.

So, when the oil droplet contacts the honeycomb film underwater, the oil cannot spread on the surface but can be absorbed by the honeycomb film. Meanwhile, the PB honeycomb film can still be considered as oleophilic underwater.

2.5 SUMMARY OF THE PROPERTIES OF HONEYCOMB FILMS

For honeycomb films prepared by the breath figure method, because the initial condensation nuclei are the same size and the growth time is the same, if the droplets do not merge together, the final pore size will be uniform.

The pore size of the honeycomb film can be increased by decreasing the substrate temperature.

Perforated honeycomb films can be prepared by increasing the hydrophilicity of the substrate.

Pincushion structure films can be obtained easily by peeling off the top layer of the honeycomb films by tape.

The underwater transparency and underwater oleophobicity of the honeycomb film and pincushion film will increase after UV-O_3 treatment.

The bubbles generation from the hydrophobic honeycomb film when the oil droplet attaches the honeycomb surface underwater. Although the oil contact angle is large underwater, the hydrophobic honeycomb films are also oleophilic underwater. And this can be explained by spreading coefficient and Laplace pressure.

2.6 EXPERIMENTAL

2.6.1 PREPARATION OF THE POLYBUTADIENE HONEYCOMB AND PINCUSHION FILMS

1,2-Poly(butadiene) (PB, RB820) was kindly provided from JSR Co. Ltd., Japan and chloroform were purchased from Sigma-Aldrich (St. Louis, MO) and WAKO Chemicals Inc. (Osaka, Japan), respectively. An amphiphilic copolymer (polymer 1, Mw = 40000g·mol^{-1}) was synthesized. Honeycomb-patterned (HC) films were prepared by depositing a 5 g L^{-1} chloroform solution of PB and polymer 1 (weight ratio PB/polymer 1 = 10:1) on a polyethylene terephthalate (PET) substrate of size 10 × 30 cm^2 under humid conditions (relative humidity ca. 90% and velocity 130L·min^{-1}) and ambient temperature.

Pincushion-patterned (PC) films were prepared by peeling off the top layer of the honeycomb film using a sheet of adhesive tape. The PET substrates with the microstructured polymer films were then cut into 1 × 1 cm^2 size pieces. As a control experiment, a flat film was prepared.

2.6.2 PREPARATION OF THE PERFORATED HONEYCOMB FILMS

1,2-Poly(butadiene) (PB, RB820) was kindly provided by JSR (Japan), and chloroform was purchased from Sigma-Aldrich (St. Louis, MO) and Fujifilm Wako Chemicals (Osaka, Japan). An amphiphilic copolymer (polymer 1, Mw= 40 kg mol^{-1}) was synthesized according to the method reported in the literature. HC-patterned films were prepared by depositing a 10–20 mL of 1–2 g L^{-1} chloroform solution of PB and polymer 1 (weight ratio PB/polymer 1 = 10:1) onto a PET substrate (10 × 30 cm2) under humid conditions (relative humidity≈90% and velocity 130 L min^{-1}) and ambient temperature.

2.6.3 HYDROPHILIC TREATMENT OF THE HONEYCOMB AND PINCUSHION FILMS

An ultraviolet and ozone exposure method (OC-250615-D+A; IWASAKI DENKI, Co. Ltd., Tokyo, Japan) was used for the hydrophilic treatment of the films. As

prepared HC and PC films were placed in the exposure chamber and treated with UV−O_3 for 30min and 60min at ambient temperature and pressure. Both the treated HC and PC films were examined using a field-emission scanning electron microscope (S-5200; Hitachi, Tokyo, Japan).

The flat PB honeycomb abbreviated as HC 0. And HC and PC films treated with UV−O_3 for 30min and 60min abbreviated as HC 30, HC 60, PC 30 and PC 60. Because the PB is a kind of rubber, it is hard to peel off the top layer with tape before oxidation.

2.6.4 CHARACTERIZATION OF MEMBRANE PHYSICAL PROPERTIES

The obtained HC and PC structures were examined with a scanning electron microscope (SEM, S-5200, Hitachi Hitech, Japan). The sample spacemen were sputtered by Os for 10 s to ensure the electrical conductivity before observation. Optical micrographs of HC films were performed by using a digital optical microscope (Keyence, Japan). The transmittance of the honeycomb and pincushion films was measured using UV-vis spectroscopy (Jasco, V-600s, Japan).

2.6.5 CONTACT ANGLE MEASUREMENT

Water and decane contact angles were recorded with a drop-shape analysis system equipped with a video camera (DM300, Kyowa Interface Science, Niiza, Japan). Whole films were placed on the horizontal surface. The static contact angles were measured on a horizontal plane.

CHAPTER 3. OIL WATER MIXTURE SEPARATION

In recent years, oil spill accidents have occurred frequently, causing great damage to the environment and causing significant economic losses. Conventional separation methods to oily wastewater discharged from our daily life and industries such as centrifugal separation, flotation, gravity separation, and electrolysis separation. Although most of the processes have been applied to actual oil-water separation, traditional methods also have limitations such as low separation efficiency, secondary pollution, slow separation speed and high cost. These shortcomings limit the development of these traditional crafts.

Inspired by natural organisms, a large number of artificial superhydrophobic materials have been prepared for oil-water separation by imitating the structure and composition of biological surfaces such as lotus leaf surfaces and water strider legs. Although various hydrophobic and oleophilic materials have been developed and proved very promising in selective oil/water separation, a water barrier forms between the filter material and the oil layer, hindering the filtration process. In contrast, hydrophilic and oleophobic materials that can selectively let water pass through, but it is theoretically difficult to prepare materials that exhibit both hydrophilic and oleophobic properties. Inspired by Nepenthes pitcher plants, people fabricate the hydrophobic membrane with oil lubricating layers and inspired by fish scales, people fabricate the hydrophilic membrane with water lubricating layers. A lot of "water-removing" filters have been fabricated by developing materials with superhydrophilicity and underwater superoleophobicity. The separation of oil and water by gravity is an important technology to purify industrial wastewater and to separate oil spills in the sea. Porous membranes are widely applied in oil-water separation. The wettability control of the membrane to oil and water is very important. The hydrophobic-oleophilic membranes can be used when the density of oil (ρ_{oil}) > 1 and the hydrophilic-oleophobic membranes can be used when $\rho_{oil} < 1$ in gravity-driven system. The wettability of membranes to oil and water depends on the structure of the membrane and the surface energy of the material. Therefore, it is necessary to achieve a surface structure and wettability suitable for oil-water

separation. Several oil-water separation membranes have been reported so far, but they have problems such as poor separation efficiency due to non-uniform pore size or oil-water separation only under specific conditions due to lack of appropriate wettability control. Therefore, separation membranes with uniform pore size and appropriately controlled wettability have been required.

In this thesis, perforated hydrophobic polybutadiene (PB) honeycomb films were fabricated with breath figure method, and then, the surface wettability was controlled by UV-O_3 treatment. Perforated HC films with controlled wettability form water or oil lubricating layers inside of the films and by prewetting treatment with water or oil, the perforated HC film can separate different liquids according to their densities. Surface wettability control based on theoretical models and relationship between oil/water separation properties and surface wettabilites of HC film are discussed.

3.1 PREPARATION AND PROPERTIES OF HONEYCOMB FILM

3.1.1 PREPARATION OF HONEYCOMB FILM

Figure 3-1 shows a schematic of the mesh-reinforced HC films, as obtained by the breath figure method. A polymer solution was cast onto a glass substrate under humid conditions, and water droplets condensed onto the surface of the solution. The condensed water droplets were packed by the capillary force among them, and close-packed water-drop arrays spontaneously formed. After the solvent and template water droplets were evaporated, a HC film eventually formed. When the film was sufficiently thin for the template water droplet to be attached to the substrate, pores in the HC film provided a path from the surface to the bottom side.

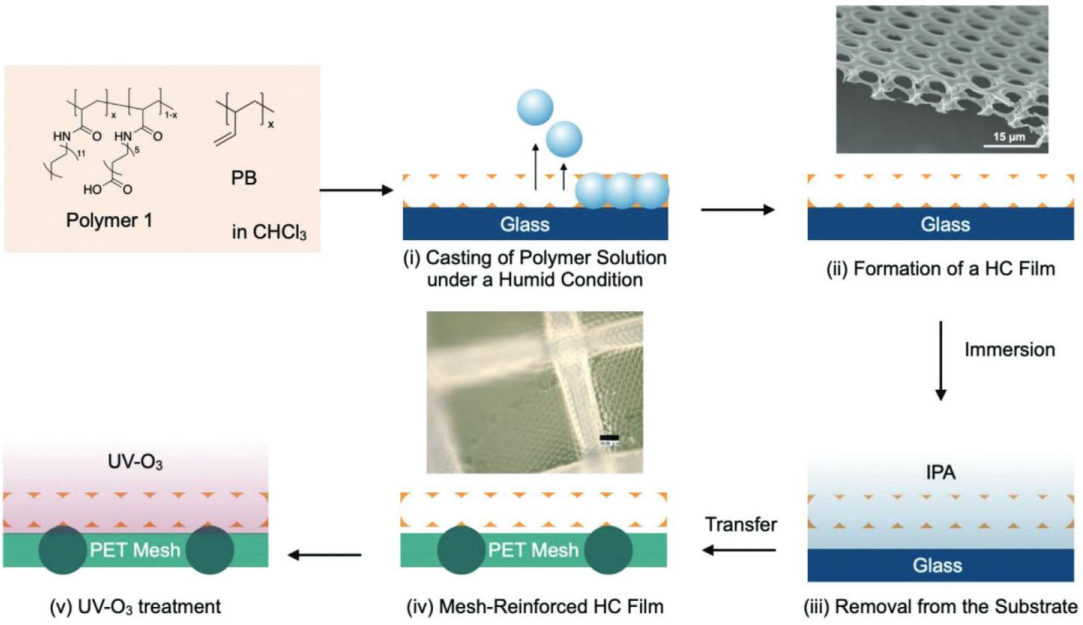

Figure 3-1. Schematic of the preparation of mesh-reinforced HC films via the breath figure method.

In order to contact the template water droplets to the substrate, the film thickness must be less than the water droplet size. This situation can be achieved by reducing the polymer concentration from typically 5–10 g L^{-1} to 1–2 g L^{-1}. Due to this solid polymer volume reduce, the thickness of the film decreased less than the diameters of water droplets and the film was eventually perforated after evaporation of solvent and template water droplet evaporation. After the samples were immersed in isopropyl alcohol (IPA), the IPA penetrated the interface between the HC film and the glass substrate; the HC film was then easily detached from the glass substrate. The removed HC film was transferred onto the PET mesh. After the film was dried at room temperature, the mesh-reinforced HC film was obtained. The average size of the pores was 10 μm, and the samples were labeled as PB, PB15, PB30, and PB45 whose UV–O_3 treatment times were 0, 15, 30, and 45 min, respectively. Since we used 1,2-polybutadiene as a main polymer, which is well-known as a synthetic rubber, due to its elastic property, the film can resist mechanical deformation and elongation.

3.1.2 THE FT-IR ATR OF HONEYCOMB FILMS

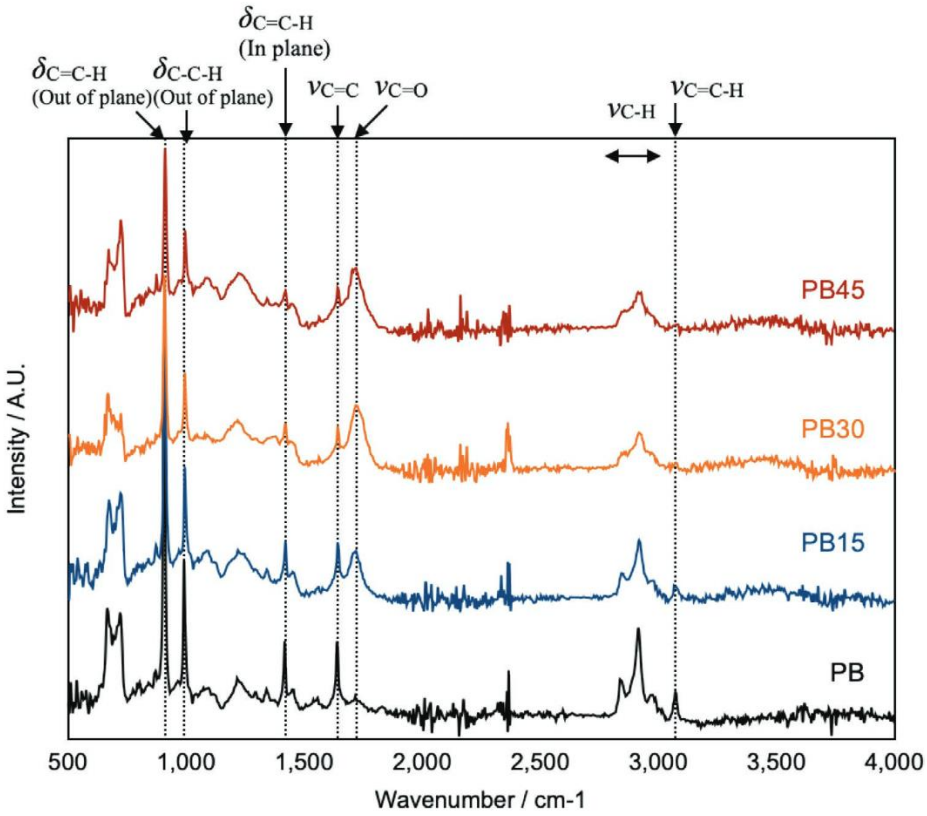

Figure 3-2. FT-IR ATR spectra of PB, PB15, PB30, and PB45 HC-patterned films.

From FT-IR ATR spectroscopy, the surface vinyl groups were gradually degraded to carbonyl and hydroxyl groups with increasing the UV-O_3 treatment time (Figure 3-2).

Before the UV–O3 treatment, peaks at 1093, 1220, 1419, and 1642 cm−1, which are attributed δ_{C-C-H} (out of plane), δ_{C-C-H} (out of plane), $\delta_{C=C-H}$ (in plane), and $\nu_{C=C}$, respectively, were clearly observed. Also, a $\nu_{C=C-H}$ peak was observed at 3062 cm−1. With increasing UV–O3 treatment time, the intensity of the peak at 1642 cm−1, which is attributed to $\nu_{C=O}$, gradually increased and the intensities of the other peaks gradually decreased. The broad ν_{O-H} band at 3400–3600 cm−1 also gradually increased in intensity.

These results indicate that hydrophilic moieties were introduced by oxidation of the HC film surfaces.

From X-ray photoelectron spectroscopy (XPS) reported in the previous report, -C=O, -COOH, and C-OH moieties formed after UV–O_3 treatment [122]. The FT-IR ATR results were well matched with this XPS measurement result.

3.1.3 THE CONTACT ANGLE WITH PB HONEYCOMB FILMS

In order to study the relationship between wettability and oil-water separation, it is necessary to measure not only the water contact angle in the air and the oil contact angle in the air, but also the water contact angle in the oil and the oil contact angle in the water. After I prepared the perforated PB honeycomb film with glass as the substrate, instead of transferring it to the PET mesh, I directly hydrophilized the films with UV-O_3 and measured their contact angles. Because the PET mesh is flexible, and it is difficult to measure the contact angle on it.

And the images of the contact angle were shown in **Figure 3-3**.

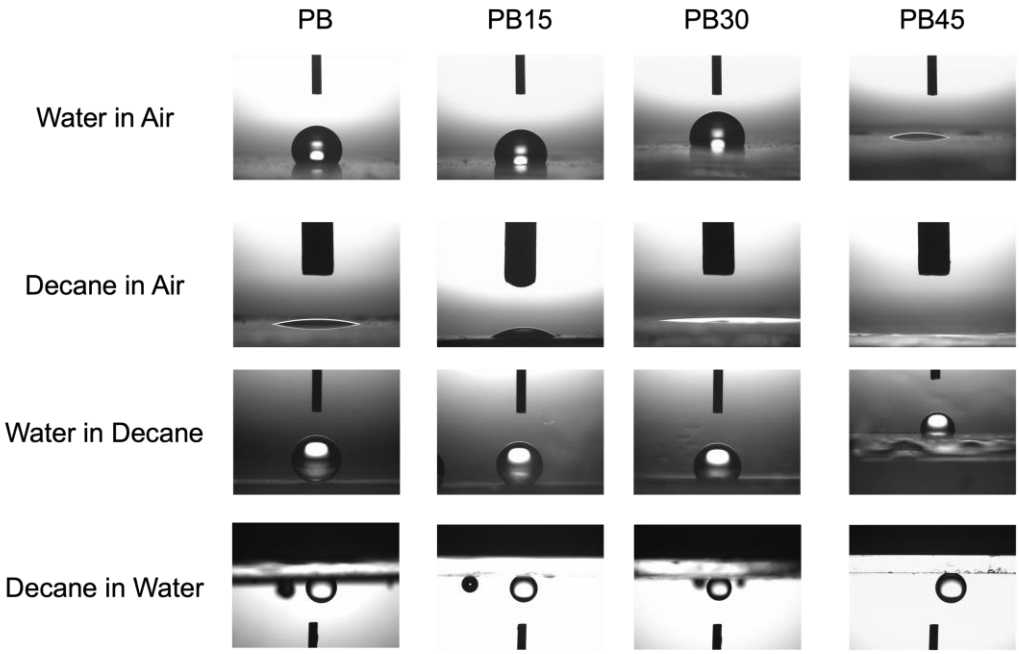

Figure 3-3. The contact angle of PB, PB15, PB30 and PB45.

We can see there are some droplets (actually these are bubbles) occurred in the images of the decane contact angle in water with PB, PB15 and PB30. After some bubbles appeared, the volume of the oil droplets decreased, indicating that the oil droplets were sucked into the honeycomb structure, which indicated that the honeycomb membrane was oleophilic. Although the decane contact angle is still large on the hydrophobic honeycomb film, the oil droplet can be absorbed in the honeycomb structure as I mentioned in Chapter 2-5. Therefore, the hydrophobic surface underwater is still oleophobic and I marked the underwater contact angle of the decane as 0° with the hydrophobic honeycomb films that can absorb oil droplets underwater.

Table 3-1. Water and oil contact angles on honeycomb films. Θ_{wa}: water CA in air, Θ_{oa}: oil (decane) CA in air, Θ_{wo}: water CA in oil (decane), Θ_{ow}: oil (decane) CA in water

	$UV\text{-}O_3$ [min.]	Θ_{wa} [°]	Θ_{oa} [°]	Θ_{wo} [°]	Θ_{ow} [°]
PB	0	123.0	16.9	169.3	absorbed
PB15	15	116.8	34.4	150.1	absorbed
PB30	30	106.0	~0	126.9	absorbed
PB45	45	~0	~0	112.8	165.2

Table 3-1 shows the data of the contact angle and “absorbed” means the oil can be absorbed by the HC film underwater. For the oil-water separation process, the film let the oil pass through. So, it makes sense to write the oil contact angle underwater as 0° with PB, PB15 and PB30 as shown in Figure 3-4.

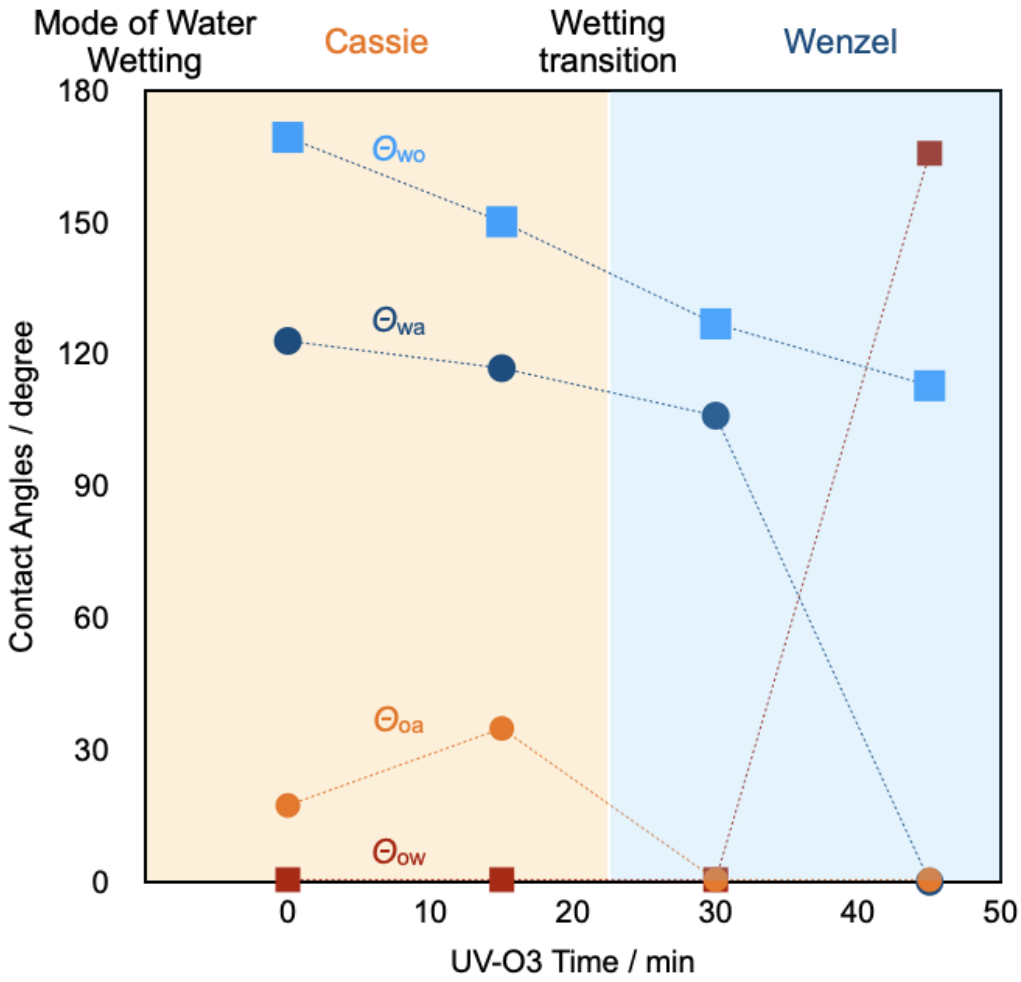

Figure 3-4. Contact angle and mode of water wetting

Figure 3-4 and Table 3-1 show the effect of UV-O_3 treatments on water and oil contact angles. After the UV-O_3 treatment of PB HC films, the contact angles of water and oil droplets in air (Θ_{wa}, Θ_{oa}), water droplets in oil (Θ_{wo}) and oil droplets in water (Θ_{ow}) were measured. Firstly, the effect of UV-O_3 treatment time on $\Theta_{wa}$was examined. As shown in Figure 3-4, Θ_{wa} gradually decreased with increasing UV-O_3 treatment time, reaching a state of complete water wetting and spreading after 45 minutes of treatment (blue dots). FT-IR results show that the peak intensity of hydrophobic alkyl groups decreases, and hydrophilic carbonyl groups increase on the surface of the film. The sudden decrease of the contact angle after 45 minutes of UV-O_3 treatment is attributed to the capillary force of the pore structure, which causes water droplets to spread through the pores when the contact angle is below 90°. Θ_{oa}increased

slightly after 15 minutes of treatment, but after that the droplets almost spread. These results indicate that the introduction of surface functional groups by UV-O_3 treatment allows the HC films to acquire amphiphilic properties.

Θ_{wa} decreased rapidly after 45 min of UV-O_3 treatment, while Θ_{wo} decreased linearly with UV-O_3 treatment time. This is related to the structure of the HC film, which is wetted by both water and oil in air after 45 minutes of treatment. Θ_{oa} is initially lower than that of water, suggesting that the HC film has a higher affinity for oil than for water. Therefore, when the environment is filled with oil, the vacancies of the HC film are filled with oil, forming a hydrophilic polymer-oil hybrid surface at the interface with the water droplets. In such a case, the water droplet contact angle in oil depends on the simple Cassie's equation (3-1).

$$\cos\Theta_{ow} = \emptyset_o \cos\Theta_{oa} + \emptyset_{polymer} \cos\Theta_{polymer} \qquad (3-1)$$

where, Θ_{ow}, Θ_{oa}, and $\Theta_{polymer}$ are contact angles of oil in water, oil in air, and oil on flat polymer, and $\emptyset_o$ and $\emptyset_{polymer}$ are surface area fraction of oil and polymer, respectively. In this process, $\Theta_{polymer}$ and $\emptyset_o$ and $\emptyset_{polymer}$ remain constant, and Θ_{oa} gradually decreases, so Θ_{ow} is considered to have decreased.

Furthermore, when the contact angle of oil droplets in water was measured on untreated or up to 30 minutes of UV-O_3 treatment, their size gradually decreased, and they were absorbed by the film after oil droplets were attached to the surface. As reported in our previous paper, the water-repellent PB HC film is not wetted with water and an air layer is maintained in the pores. The pores of the HC film are connected by transverse holes, which allow the oil droplets to be absorbed by the volume of the pores. On the other hand, when the hydrophilicity of the HC film increased and the pores were wetted by water, the interface with the oil droplets became a mixture of water and hydrophilic polymer surface, as shown in Cassie's equation (3-1), and Θ_{ow} showed a high contact angle in the case of 45 min UV-O_3 treatment.

As mentioned before, Aizenberg *et al.* developed a slippery liquid-infused porous surface (SLIPS) inspired by Nepenthes pitcher plants. The hydrophobic surface wetted by oil will be more hydrophobic. As the table 3-1 shows, the water contact angle in oil is larger than the water contact angle in air with the hydrophobic honeycomb films (PB, PB15 and PB30). As mentioned before, fish scales will change from oleophilic in air to oleophobic underwater. When the environment is filled with water, the vacancies of the PB45 film are filled with water, forming an oleophilic polymer-water hybrid surface at the interface with the oil droplets. And PB45 change from oleophilic to underwater oleophobic. So, the Θ_{ow} rapidly increasing after 45 min of UV-O_3 treatment.

3.2 RESULTS OF OIL-WATER MIXTURE SEPARATION

In this thesis, I prepared perforated PB, PB15, PB30 and PB45 on PET mesh for oil water separation. The results of oil water separation were shown in **Table 3-2.** This is the first report about application of HC films to liquid separation membranes.

Table 3-2 Contact angle an oil water separation result.

Sample	Polymer	UV-O_3 [min.]	ϕ [μm]	$\theta_{w/a}$ [°]	$\theta_{o/a}$ [°]	$\theta_{w/o}$ [°]	$\theta_{o/w}$ [°]	W→O (ρ_o/ρ_w<1)	W→O (ρ_o/ρ_w>1)	O→W (ρ_o/ρ_w<1)	O→W (ρ_o/ρ_w>1)
PB	PB	0	10	123.0	16.9	169.3	Abs.	-	O	O	O
PB15	PB	15	10	116.8	34.4	150.1	Abs.	-	O	O	O
PB30	PB	30	10	106.0	0	126.9	Abs.	W	W	O	O
PB45	PB	45	10	0	0	112.8	165.2	W	W	O	O

It shows that amphiphilic perforated PB45 HC films with controlled wettability offer realizing membranes that can separate different liquids according to their densities by changing initial liquid added into the surface of the PB45 film. And hydrophobic PB can separate oil-water mixture when the density of oil lager than water.

3.2.1 OIL REMOVING METHOD SEPARATION WITH PB

As mentioned before, oil contact angle underwater and water contact angle in oil are also important for determining whether oil and water can be separated.

The PB is hydrophobic and oleophilic, and these two wetting properties are necessary oil-water mixture separation with oil-removing method. And the images before and after adding oil were shown in Figure 3-5 and Figure3-6.

Dyed 1,2,4-Trichlorobenzene (TCB) ($\rho_O > 1$) blue. When pour water, the water will be repelled on the PB membrane because of its hydrophobicity. Then we pour the TCB, and it can pass through the PB membrane even in the presence of a water barrier layer. Therefore, the PB can separate TCB and water with the oil removing method as shown in Figure 3-5.

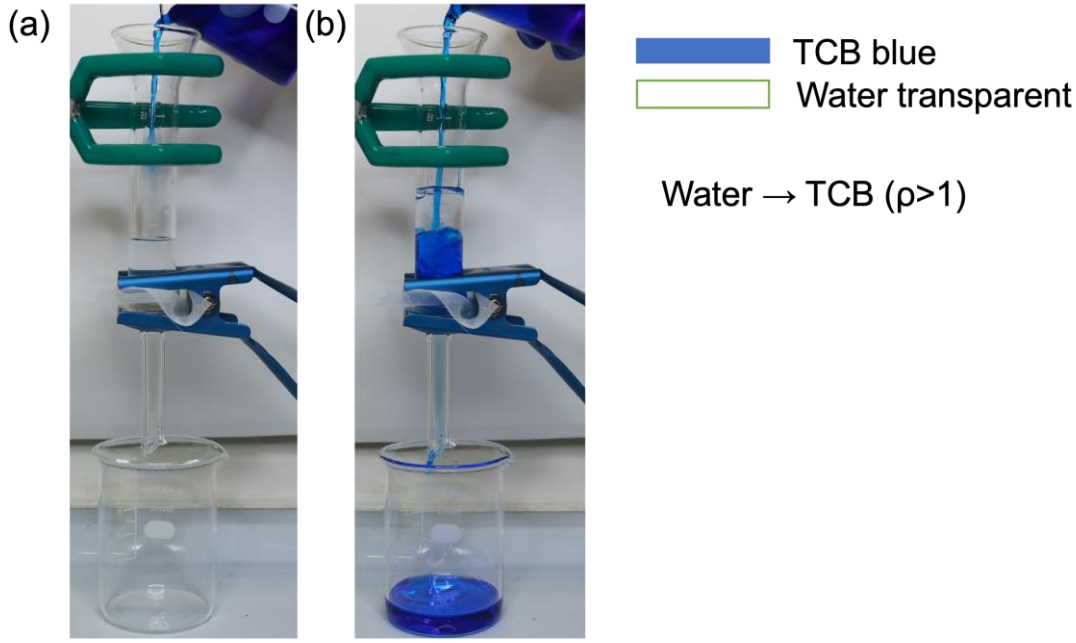

Figure 3-5. Oil water separation with PB. The TCB is blue-colored, and the water is transparent. (a) Pour water on the PB, and water was kept repellent from the PB HC film, then pour the TCB. (b) The TCB and was separated from the mixture and only oil was trickle down into the bottom flask.

In oil-water separation, there are many kinds of oil, so after separating TCB-water mixture, other oils also need to be measured. Dyed water green with copper sulfate, and the transparent oil is Perfluoromethylcyclohexane (C_7F_{14}) ($\rho_O > 1$). Firstly, when water was poured onto the filter made from PB sample, water did not go through the filter due to high water repellency of the PB HC film. Then pouring the C_7F_{14}, and it can pass through the PB membrane even in the presence of a water barrier layer. Therefore, the PB can separate C_7F_{14} and water with the oil removing method as shown in Figure 3-6.

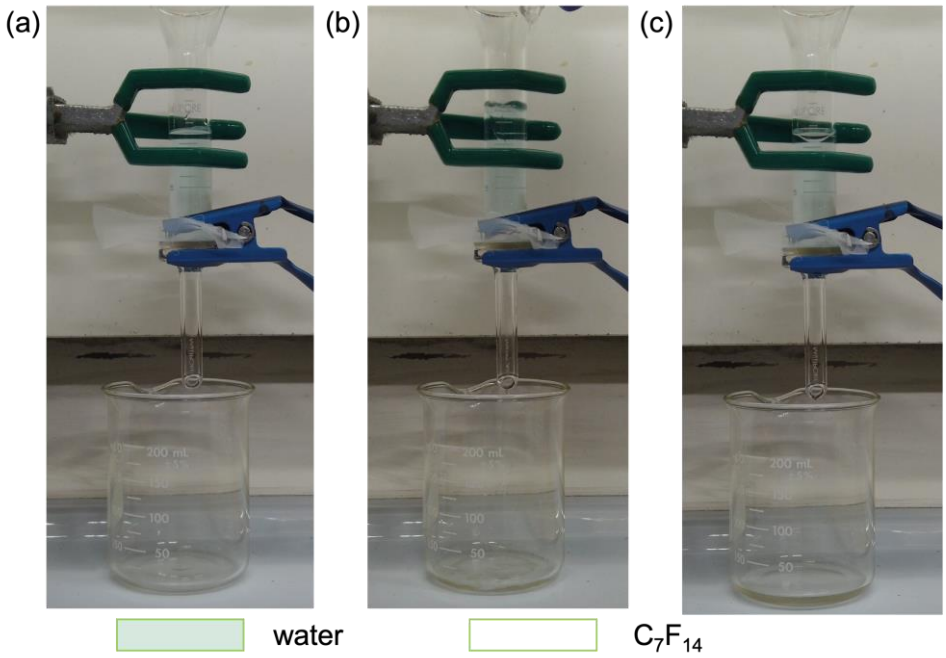

Figure 3-6. Oil water separation with PB. The water is green-colored, and the C_7F_{14} is transparent. (a) Pour water on the PB, and water was kept repellent from the PB HC film, then pour the C_7F_{14}. (b) The C_7F_{14} was separated from the mixture and only C_7F_{14} was trickle down into the bottom flask c) After all the C_7F_{14} has passed through, the water was still kept repellent on the PB membrane.

In addition, there are Cu^{2+} in water and the oil-water mixture is still successfully separated. Therefore, oil in seawater (contains salt) also can be expected to be separated.

PB HC membrane has the same disadvantage as other oil removing separation membranes, when the density of oil is less than water, oil water cannot be separated because oil cannot reach the membrane because of water barrier (Figure 3-7). Dyed decane ($\rho_O < 1$) blue. When pour the decane, the decane can pass through the PB because of its oleophilicity. Then pour the water, and we can see the water can form a water barrier layer at the bottom of the liquid. Because PB is hydrophobic and the density of decane is less than water, both the water and decane cannot pass through the surface.

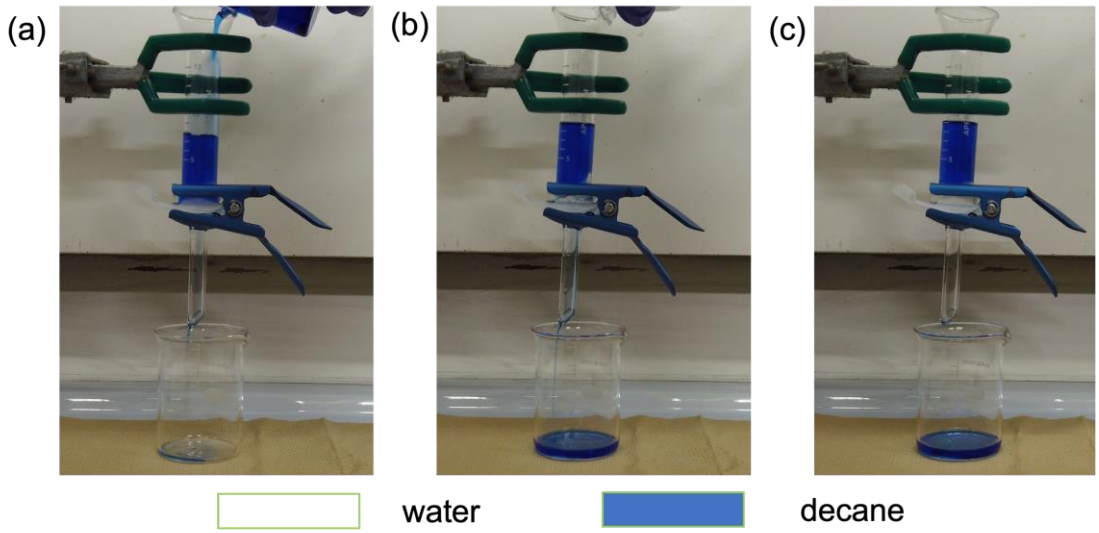

Figure 3-7. Oil water separation with PB. The decane is blue-colored, and the water is transparent. (a) Pour the decane and it can pass through the PB membrane. (b) Pour the water. c) Water and decane are repelled on the PB membrane.

3.2.2 OIL-WATER MIXTURE SEPARATION WITH PB45

Inspired by fish scales, the hydrophilic surface can change from oleophilic in air to oleophobic underwater. The PB45 HC film is superhydrophilic and superoleophilic with 45 min UV-O_3 treatment. Meanwhile PB45 also has the special wettabilities that oleophobic underwater and hydrophobic in oil as mentioned before.

I tried to separate water and oil with using water and different density oils through the mesh-reinforced PB45 HC films. Dyed the TCB ($\rho_o > 1$) and decane ($\rho_o < 1$) blue. When the density of oil (TCB) large than water, wet the PB45 with TCB and then pour water. The TCB can pass through the PB45 and form an oil lubricating layer so that the water can be repelled on the PB45 (Figure 3-8a). And when the density of oil (decane) less than water, wet the PB45 with water and then pour decane. The water can pass through the PB45 and form a water lubricating layer so that the decane can be repelled on the PB45 (Figure 3-8b).

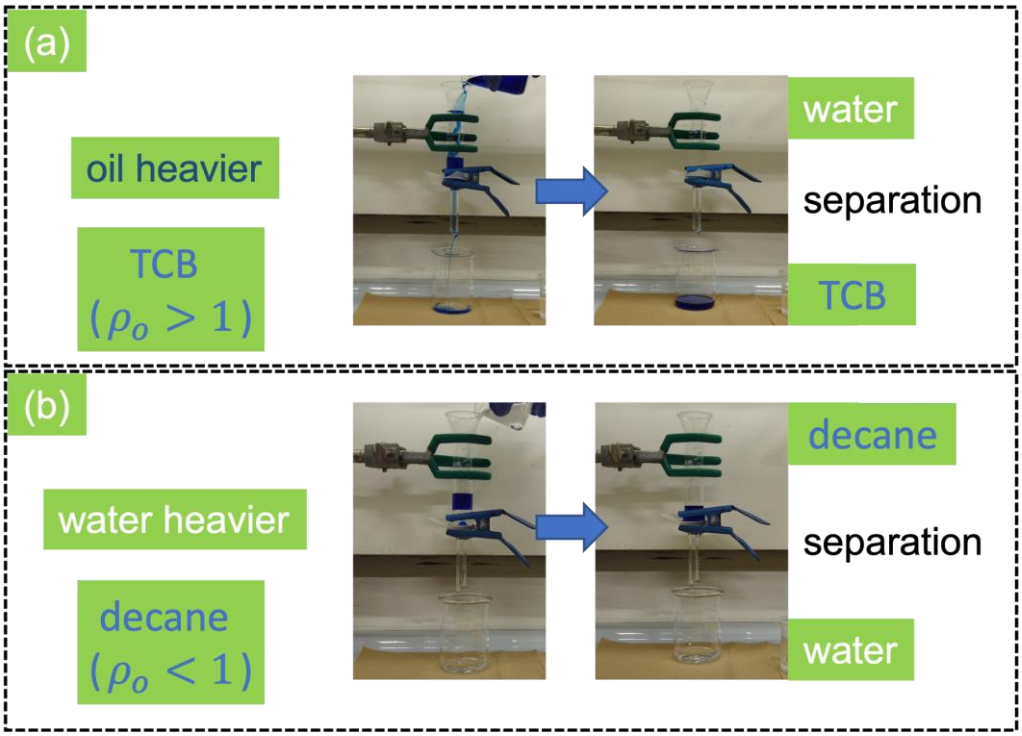

Figure 3-8. Oil water separation with PB45. The TCB and decane are blue-colored and the water is transparent. (a) Wet PB45 with TCB and then TCB-water can be separated. (b) Wet PB45 with water and then decane-water can be separated.

Through the experimental results, we can know that the wettability of the film is indeed changed by the wetting of different liquids (oil or water), and this wettability change can be used for oil-water separation by forming a lubricating layer. In addition to separating TCB and decane, I also performed separation

experiments on hexadecane ($\rho_O < 1$) and C_7F_{14} ($\rho_O > 1$). Table 3-3 show that for different oils, the membrane can be used for oil-water separation.

Table 3-3. Separation of different oil-water mixtures with PB45.

Oil	Density (g/mL)	$\Upsilon_{oil-air}$ ($mN \cdot m^{-1}$)	Υ_{oil-H_2O} ($mN \cdot m^{-1}$)	Separation
Decane	0.73	24	50	√
Hexadecane	0.77	27	52	√
TCB	1.46	39	45	√
C_7F_{14}	1.80	13	58	√

Separation of different oils is important, and both PB and PB45 have been successful even though PB can only separate with heavier oil (TCB and C_7F14)

3.2.3 MECHANISM OF OIL WATER SEPARATION

When we know that honeycomb membranes can be used in oil-water separation, the amount of liquid that can be supported on the membrane is also very important. For porous membranes, as long as the pressure is higher than the critical intrusion pressure, the liquid will eventually penetrate the porous structure.

3.2.3.1 THE INTRUSION PRESSURE OF HONEYCOMB FILMS

The analysis shows that the oil-water separation efficiency is determined by the surface wettability. This can be explained from the view of capillary force between oil and water (Figure 3-9 a, b). If the liquid is water, an upward capillary force is formed when the porous membrane is superhydrophobic (Figure 3-9a). When the membrane is hydrophilic, water wets the porous membrane completely, forming downward capillary force (Figure 3-9b), which allows water penetration and repels the oil.

The first analysis of intrusion pressure is attributed to Lucas and Washburn. [132,133] The intrusion pressure is determined by the balance between the static pressure and the capillary pressure.

The capillary pressure ΔP is given by the Laplace law $\Delta P = \frac{2\Upsilon}{R}$.

The theoretical intrusion pressure (ΔP_{the}) can be calculated using the following equation which has been widely applied to oil-water separation field [134-137]

$$\Delta P_{the} = -\frac{2\Upsilon_{12}\cos\Theta}{d} \qquad (3-2)$$

where Υ_{12} is the interfacial tension between two phases, d is the pore size of the HC film.

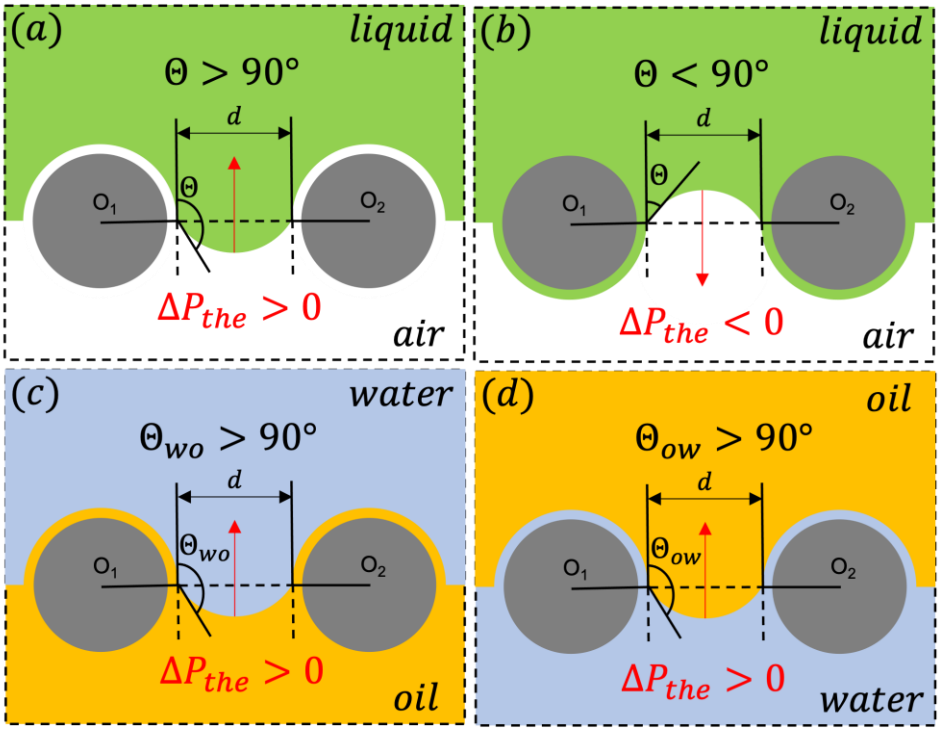

Figure 3-9. Schematic diagrams of the wetting model of porous materials for oil/water separation.

For the water on hydrophobic PB HC membrane, the $\cos\Theta_{wa} < 0$, so the $\Delta P_{the} > 0$. This is consistent with the experiment result that the water cannot pass through the PB. And the decane on oleophilic PB HC membrane, the

$\cos\Theta_{oa} > 0$, so the $\Delta P_{the} < 0$. That is to say the decane will pass through the PB without any applied pressure. This is consistent with the experiment result that the decane can pass through the PB. (Figure 3-9 a, b)

The PB45 is amphiphilic, the oil or water on the PB45 is like the scheme in Figure 3-9b. The theoretical water intrusion pressure in oil of PB45 can be written into

$$\Delta P_{the} = -\frac{2\Upsilon_{wo}\cos\Theta_{wo}}{d} \qquad (3-3)$$

where Υ_{wo} is the interfacial tension between water and oil, $\cos\Theta_{wo}$ is the water contact angle in oil, d is the pore size diameter of the HC film.

The theoretical oil intrusion pressure underwater of PB45 can be written into

$$\Delta P_{the} = -\frac{2\Upsilon_{ow}\cos\Theta_{ow}}{d} \qquad (3-4)$$

where Υ_{ow} is the interfacial tension between water and oil, $\cos\Theta_{ow}$ is the oil contact angle underwater, d is the pore size diameter of the HC film.

For the PB45, the $\cos\Theta_{wo} < 0$, so the $\Delta P_{the} > 0$. The water cannot pass through the PB45 after it wetted oil. And the $\cos\Theta_{ow} < 0$, so the $\Delta P_{the} > 0$. That is to say the oil also cannot pass through the PB45 after it wetted by water This is consistent with the experiment result that the decane can pass through the PB. (Figure 3-9 c, d)

3.2.3.2 THE HEIGHT OF LIQUID CAN SUPPORT ON PB AND PB45

As the intrusion pressure arises from the weight of liquid on the surface, the experimental intrusion pressure (ΔP_{exp}) was calculated using equation

$$\Delta P_{exp} = \rho g h_{max} \qquad (3-5)$$

where ρ is the density of the liquid, g is the acceleration of gravity, and h_{max} is the maximum height of the liquid that the HC film can support.

The interfacial tension of water and air (Υ_{wa}) is 72.8 mN/m^{-1}. The water contact angle in air on PB is 123.0°. Substitute these values into the equation (3-2) and obtain the water intrusion pressure on PB is

$$\Delta P_{the} = -\frac{2\Upsilon_{wa}\cos\Theta_{wa}}{d} = -\frac{2\times 72.8\times 10^{-3}\cos 123.0°}{10\times 10^{-6}} \approx 7.9kPa$$

Substitute the value of intrusion pressure into the equation (3-5) and obtain the height of water $h_{max} \approx 0.78m$.

The interfacial tension of decane and water ($\Upsilon_{decane-water}$) is 50 mN/m^{-1}. The decane contact angle underwater on PB45 is 165.2°. Substitute these values into the equation (3-4) and obtain the decane intrusion pressure on PB45 prewetted by water is

$$\Delta P_{the} = -\frac{2\Upsilon_{decane-water}\cos\Theta_{wo}}{d} = -\frac{2\times 50\times 10^{-3}\cos 165.2°}{10\times 10^{-6}} \approx 9.6kPa$$

And the $\rho_{decane} = 0.73\ g/m^3$. Substitute the value into the equation (3-5) and obtain the height of decane is $h_{decane} \approx 1.34m$.

Compared to conventional porous separation membrane, [138-140] the intrusion pressure is high for the small pore size and high oil contact angle underwater.

Table 3-4. The intrusion pressure comparison with different membranes.

Sample	Intrusion pressure (kPa)	Ref.
PB45 HC	9.6	this work
SH-ZIF-67/copper mesh	2.6	[138]
zeolite-coated mesh	0.729	[139]
palygorskite coated mesh	1.5	[140]

3.2.4 SEPARATION AND WITH PB15 AND PB30

The wettability of PB15 and PB30 is between PB and PB45. From the separation results shown before in the **Table 3-2,** we can see that PB15 and PB are suitable for the same separation, and PB30 and PB45 are suitable for the same separation.

For PB15, compared with PB, after the coating is prepared, UV-O_3 treatment is required, and there are no properties better than PB, so in these series of layers, PB15 is not as practical as PB.

Even though the PB30 and PB45 are suitable for both water removing method and oil removing method, the PB30 is still hydrophobic, so water must not pass through it as fast as the superhydrophilic PB45. So, in these series of layers, PB30 is not as practical as PB45.

But these two HC films are very important and valuable for the study of the wettability transition and the penetration condition of water on the perforated HC films.

3.2.4.1 SEPARATION AND WITH PB15

The HC film is also hydrophobic after 15 min UV-O3 treatment. The hydrophobic and oleophilic PB15 can separate TCB and water with the oil removing method. Dyed the TCB blue. When pour water, the water will be

repelled on the PB membrane because of its hydrophobicity. Then we pour the TCB, and it can pass through the PB membrane even in the presence of a water barrier layer. Therefore, the PB can separate TCB and water with the oil removing method as shown in Figure 3-8.

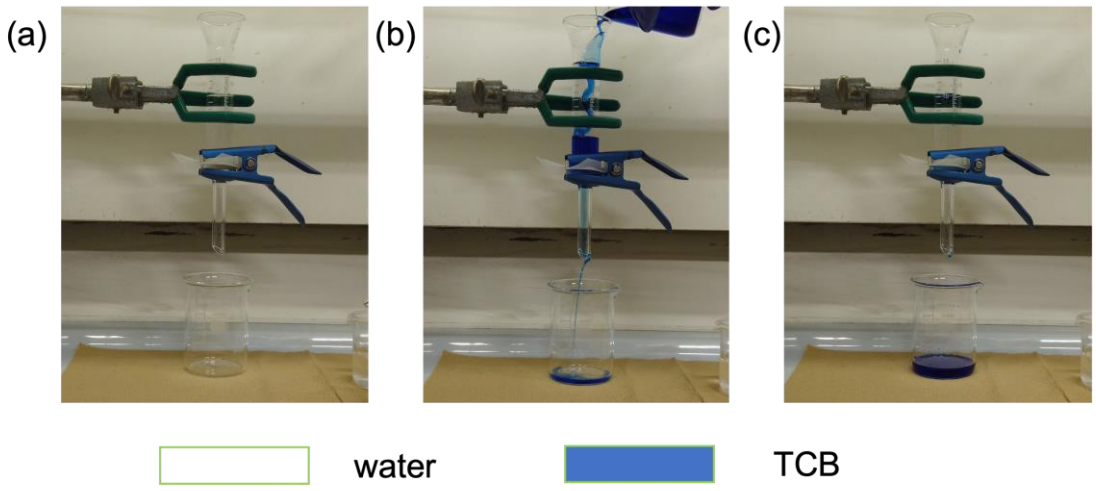

Figure 3-10. Oil water separation with PB15. The TCB is blue-colored, and the water is transparent. (a) Pour water on the PB15. (b) Pour the TCB. c) After all the TCB has passed through, the water is stilled repelled on the PB15 membrane.

PB15 has the same disadvantage as other oil removing separation membranes, when the density of oil is less than water, oil water cannot be separated because oil cannot reach the membrane because of water barrier.

3.2.4.2 SEPARATION AND WITH PB30

The PB30 is still hydrophobic and oleophilic. So, PB30 should also work for oil removing separation method. That is to say, the PB30 should repel water if it is poured first. But in fact, the water pass through the surface.

I compared the results of PB30 with other hydrophobic HC films. Firstly, when water was poured onto the filter made from PB and PB15, water did not go through the filter due to high water repellency of the PB and PB15 (Figure 3-11 (a) and Figure 3-11 (b)). But the water could pass through the PB30 as shown

in Figure 3-11(d). And then pour decane and the decane did not sink into the water due to the difference of density. Then the decane was kept repellent from PB30 films after the water passed through PB30 even though the PB30 is hydrophobic and oleophilic.

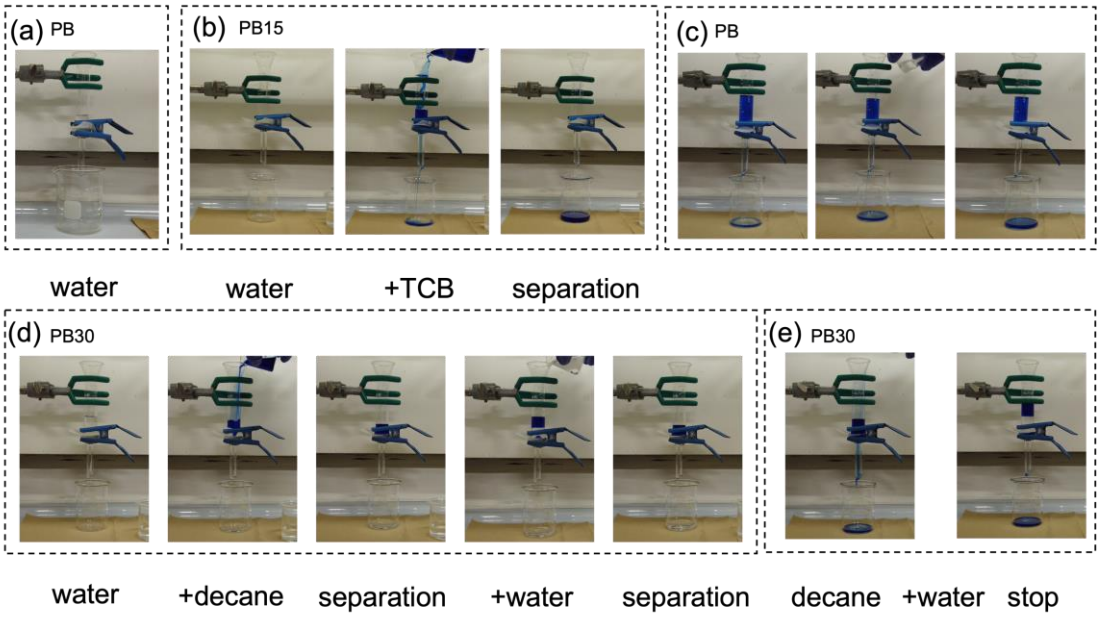

Figure 3-11. Photographs of oil water separation experiments: (a) After water was poured on PB. There is no liquid leakage. (b) PB15 w→o (decane). Only blue-colored decane was separated. (c) PB o (TCB) →w→stop. Only blue-colored TCB was separated, and after water mixing, decane float on the water. (d) PB30 w→o (decane) →w. Water was separated. (e) PB30 o (decane) →w→stop. Only blue-colored TCB was separated, and after water mixing, decane float on the water.

In the case where the TCB was poured onto the water, the water remained repelled from the PB HC film, but the oil was separated from the mixture and only the TCB trickled into the bottom flask. Because the PB and PB15 films have a low Θ_{oa} and oil was absorbed in the HC film underwater, oil was drawn into the HC film structure, and an oil lubricating layer was formed. In these cases, water could not pass through the filter, and oil could be separated. When oil was poured first, the oil lubricating layer firstly formed, as the result, only oil

can be separated in both ρ_o/ρ_w<1 (decane) and ρ_o/ρ_w>1 (TCB) cases. When pour decane first, the first oil layer can be separated but after water mixing, no more decane could not be separated since decane floated on the water due to lower density of decane than that of water (Figure 3-11 (c)).

The separating property drastically changed when the PB30 was used as the filter. In this case, the firstly poured water dropped through the filter, and oil could not go through the filter (Figure 3-11 (d)). Therefore, only water was separated. On the other hand, when the decane was poured first on the PB30, the first oil layer can be separated but after water mixing, no more decane could not be separated since decane floated on the water due to lower density of decane than that of water (Figure 3-11 (e)). Those results were completely same when PB45 sample was used as the filter.

And from the intrusion pressure equation (3-2), the water contact angle in air on PB30 is 106.0°. And the $\cos\Theta_{wa} < 0$, so the $\Delta P_{the} > 0$. That is to say the water will pass through the PB30 as the scheme shown in Figure 3-9 (a).

But for PB30, the intrusion pressure theory doesn't match the results.

3.2.5 WETTING STATE TRANSITION AND PENETRATION CONDITION OF HC FILMS

The Θ_{wa} of PB30 was 106.0˚, which is high enough to repellent the water, however, water has gone through the filter. To understand this controversy phenomenon, we checked water permeation property of HC film. Normally, PB film has high water repellency and no water permeation to the pores was found (Figure 3-18 (a)). On the other hand, water spread through the side pores of PB30 even though the Θ_{wa} was high enough. This was caused by Cassie-Wenzel transition of wetting modes. There are two modes to characterize water repellent states; one is Cassie mode shown in the equation (3-6) and the other is Wenzel mode, which shows that apparent contact angle $\Theta_{apparent}$ is enhanced by surface roughness depending on the following equation.

$$\cos \Theta\text{apparent} = r \cos \Theta\text{oa} \quad (3\text{-}6)$$

where r is a ratio between actual surface area and apparent surface area. In the Wenzel state, water adhered on the surface of substrate along to the surface roughness.

If the water cannot pass through the porous membrane, it is Cassie model and the water-droplet contact angle is expressed by the simple Cassie equation

$$\cos \Theta_C = \emptyset_{polymer} \cos \Theta_{w/a-flat} + (1 - \emptyset_{polymer}) \cos \pi \quad (3\text{-}7)$$

where $\emptyset_{polymer}$ is the surface area fraction of polymer. From these two models, the surface wettability of HC membranes can be separated as Wenzel and Cassie states depending on UV-O3 treatment times (Figure 3-18).

There is a point transition from Cassie to Wenzel with decreasing Θwa, according to an equation (3-4), which gives the penetration condition.

$$\cos \Theta_{w/a-flat} > \frac{1-\emptyset_{polymer}}{r-\emptyset_{polymer}} \quad (3\text{-}8)$$

where $\Theta_{wa-flat}$ is the water contact angle of flat film. $\Theta_{wa-flat}$ of 0 min, 15 min, 30 min and 45 min UV-O_3 treatment were 93.0˚, 64.8˚, 28.0˚, and 11.7˚, respectively (Table 3-5).

Table 3-5. The water contact angle on PB flat films and PB honeycomb films treated by UV-O3 for 0,15,30 and 45 min, respectively

UV-O_3 [min.]	$\Theta_{w/a-flat}$ [°]	Θ_{wa} [°]
0	93.0	123.0
15	64.8	116.8
30	28.0	106.0
45	11.4	~0

Since $\emptyset_{polymer}$ of HC film is normally 0.6, therefore from PB15 sample, the r value of HC film has over 1.66. The $\Theta_{wa-flat}$ decreased to 28.0˚ in the case of

PB30, which means left- and right-handed term of the equation (3-8) were 0.88 and 0.38, respectively, which eventually satisfy the equation (3-8). This result indicated that PB30 film over the penetration condition, the water eventually go through the filter. This water layer formed inside of the HC film pores, this works as an aqueous lubricating layer, which prevent the penetration of oil. On the other hand, when oil comes first, the oil has higher affinity to the HC film pores and lower surface tensions, oil layer was formed inside of the HC film and only oil was separated from the mixture. These results indicate that wetting transition of the filter is very important for effective water/oil separation membrane and these HC films with both water and oil wetting properties, which are considered as “amphiphilic” HC films, are ideal for liquid separation membranes.

Figure 3-19 is a schematic illustration of relationship between water/oil separation properties and wetting properties of HC films. In the case of Cassie state for water and low Θ_{oa} (and Θ_{ow}) cases, water was repelled from the surface of HC film, no liquid was leaked from the membrane when water came firstly (Figure 3-19, left side image). On the other hand, oil firstly poured into the membrane, oil spread into the HC pores and form a lubricating layer of oil inside of the HC film owing to low surface tension of oil (Figure 3-19, center image). This situation is considered as Wenzel state for oil and Cassie state for water. Due to high water repellency, only oil can be dropped though the membrane regardless of the oil density. Even though the water was firstly poured, oil whose density was higher than that of water can sink into the bottom of water phase, which repelled by the HC film, oil formed a lubricating layer as same as the case of oil poured first. When the equation (3-4) was filled and the wetting transition occurred, water could form lubricating layer in the HC film, water and oil can separate by just changing which liquid poured into the membrane first (Figure 3-19, right side image).

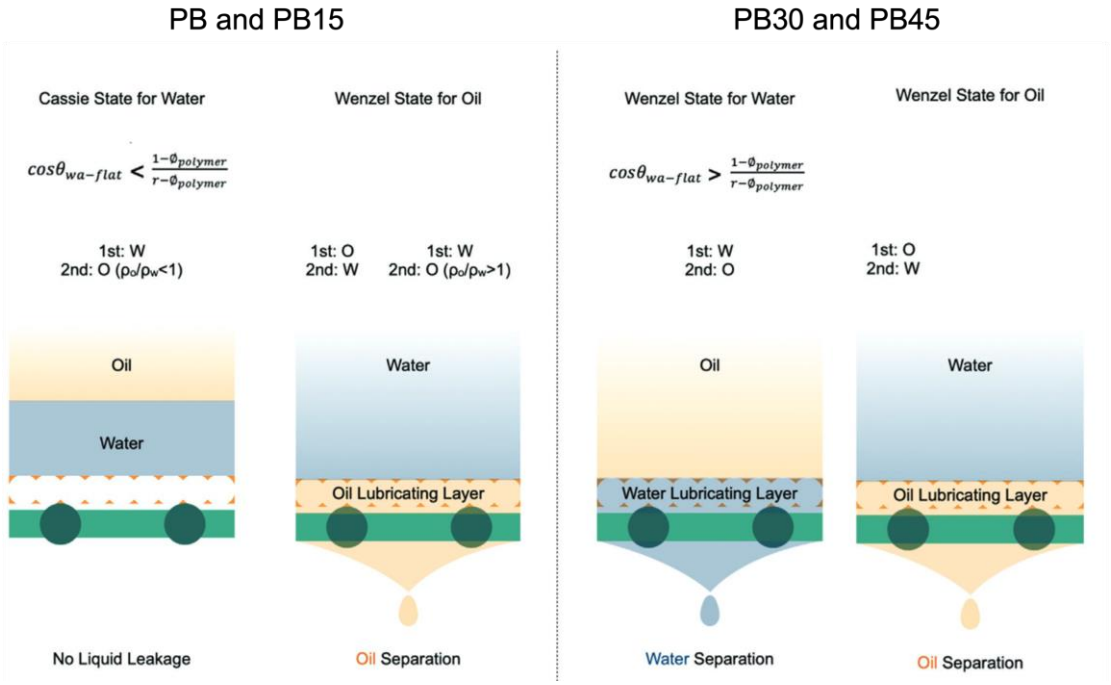

Figure 3-19. Schematic illustration of oil and water separation through amphiphilic HC films.

3.3 CREATION OF A HYDROPHOBIC SURFACE FROM A HYDROPHILIC POLYMER

The contact angle of water droplets in air, non-hydrophilized HC film was 123.1° (HC0). And this decreased to 106.5° after 30min hydrophilic treatment (HC30). After peeling off the top layer of HC30, the water contact angle is 79.4° (PC30). The water contact angle on flat polybutadiene with 30min UV-O_3 treatment is 28° (Table 3-6).

Table 3-6. Water contact angle (CA) with different films in air.

Films	Water CA (°)
HC 0	123.1±0.4
HC 30	106.5±0.5
PC 30	79.4±2.0
Flat 30	28.0±0.5

First, all three of the HC30, PC30 and Flat30 are polybutadiene treated with UV-O_3 for 30min. The Flat30 has a water contact angle far less than 65°. Nevertheless, the HC30 is still hydrophobic. I found that, increasing roughness turns hydrophilic material to hydrophobic surface. Other researchers indicate that the limit for hydrophilic materials is 65°. But in this study, the flat surface with 28° could also change to hydrophobic surface with the honeycomb structure because of the high barrier energy.

And PC30 is still hydrophilic but the hydrophilicity is not higher than Flat30.

3.4 EXPERIMENTAL

3.4.1 FABRICATION OF PERFORATED HC MEMBRANE

PB (RB820) was kindly provided by JSR (Japan), and chloroform was purchased from Sigma-Aldrich (St. Louis, MO) and Fujifilm Wako Chemicals (Osaka, Japan). An amphiphilic copolymer (polymer 1, Mw= 40 kg mol^{-1}) was synthesized according to the method reported in the literature. HC-patterned films were prepared by depositing a 10–20 mL of 1–2 g L^{-1} chloroform solution of PB and polymer 1 (weight ratio PB/polymer 1 = 10:1) onto a PET substrate (10 × 30 cm2) under humid conditions (relative humidity≈90% and velocity 130 L min^{-1}) and ambient temperature.

A UV–O_3 cleaner (OC-250615-D+A; Iwasaki Denki, Tokyo) was used for the hydrophilic treatment of the films. As-prepared HC films were placed in the exposure chamber and treated with UV–O_3 for 15, 30, or 45min at ambient temperature and pressure. Those samples were named as PB, PB15, PB30, and PB45, respectively. The film was then removed using isopropanol (EP/Fujifilm Wako Chemical Industry) and tweezers and transferred onto a PET mesh (SAN1260, Sanplatec, Osaka).

3.4.2 CHARACTERIZATION OF MEMBRANE CHEMICAL AND PHYSICAL PROPERTIES

The treated HC films were examined using an optical microscope (VHX-500, Keyence, Osaka) and a field-emission scanning electron microscope (S-5200, Hitachi, Tokyo) after the specimens were coated with Osusing anosmium sputterer (HPS-1SW, Mito). Water and decane contact angles were recorded with a drop-shape analysis system equipped with a video camera (DM300,Kyowa Interface Science, Niiza, Japan). Whole films were placed on the horizontal surface. The static contact angles were measured on a horizontal plane.

3.4.3. WATER/OIL SEPARATION EXPERIMENTS

Perfluoro(methylcyclopentane) (Tokyo Chemical Industry), 1,2,4-Trichlorobenzene (Tokyo Chemical Industry), decane (Fujifilm Wako Pure Chemical Industries) and hexadecane (Fujifilm Wako Pure Chemical Industries), whose densities (ρo) are greater than and less than that of water (ρw), respectively, were used for the experiment. The mesh-reinforced HC film was fixed onto a funnel with a glass filter as a filter membrane and was sandwiched with a glass cup with a clamp. Water or oil was poured from the top of the filter, and the liquid transported though the membrane was monitored using a video camera.

CHAPTER 4. OIL-IN-WATER EMULSION SEPARATION

Normally, oil-spills in natural environment are immiscible mixtures such as insoluble fatty glycerides and other related oil-water mixtures consisting of unstable oil droplets, free-floating oils, or stable emulsions.

For the case of crude oil leaking at sea, on the one hand, crude oil contains naphthalene, polar aromatic hydrocarbons and many amphiphilic compounds, which not only increases the viscosity of crude oil but also makes it easier to form small emulsions. On the other hand, with the long-term motion of the waves, the oil with low surface energy will be dispersed to form droplets of several microns.

The main component of crude oil can be removed by simple “oil and water” separation and honeycomb membranes are very effective. But there are small emulsions simultaneously formed, and those emulsions also should be removed.

Therefore, both "oil in water" and “oil-in-water emulsion" separation membrane are worth investigating.

4.1 HLB AND PREPARED OF OIL-IN-WATER EMULSION

Oil-in-water emulsion is a common emulsion system. It was used as the target emulsion in Griffin's classic experiment to determine the HLB (hydrophile-lipophile balance) value of various surfactants.[141]

The HLB value is called the hydrophilic-hydrophobic balance value, also known as the water-oil degree. In 1949, W.C.Griffin first proposed the HLB value, explaining the equilibrium relationship between the hydrophilic group and the oleophilic group in the surfactant molecule.[141]

Surfactant is an amphiphilic molecule with hydrophilic groups and oleophilic groups. The amount of size and force balance between the hydrophilic and oleophilic groups in the surfactant molecule is defined as the HLB value of the

surfactant. The larger the HLB value, the stronger the hydrophilicity, and the smaller the HLB value, the stronger oleophilicity. Normally, the HLB value ranges from 1 to 40. It is not only related to the hydrophilic and oleophilic properties of surfactants, but also to the surface tension of surfactants, adsorption on the interface, emulsification, and emulsion stability, etc.

The HLB value has important reference value in practical application. Lipophilic surfactants have lower HLB values and hydrophilic surfactants have higher HLB values.

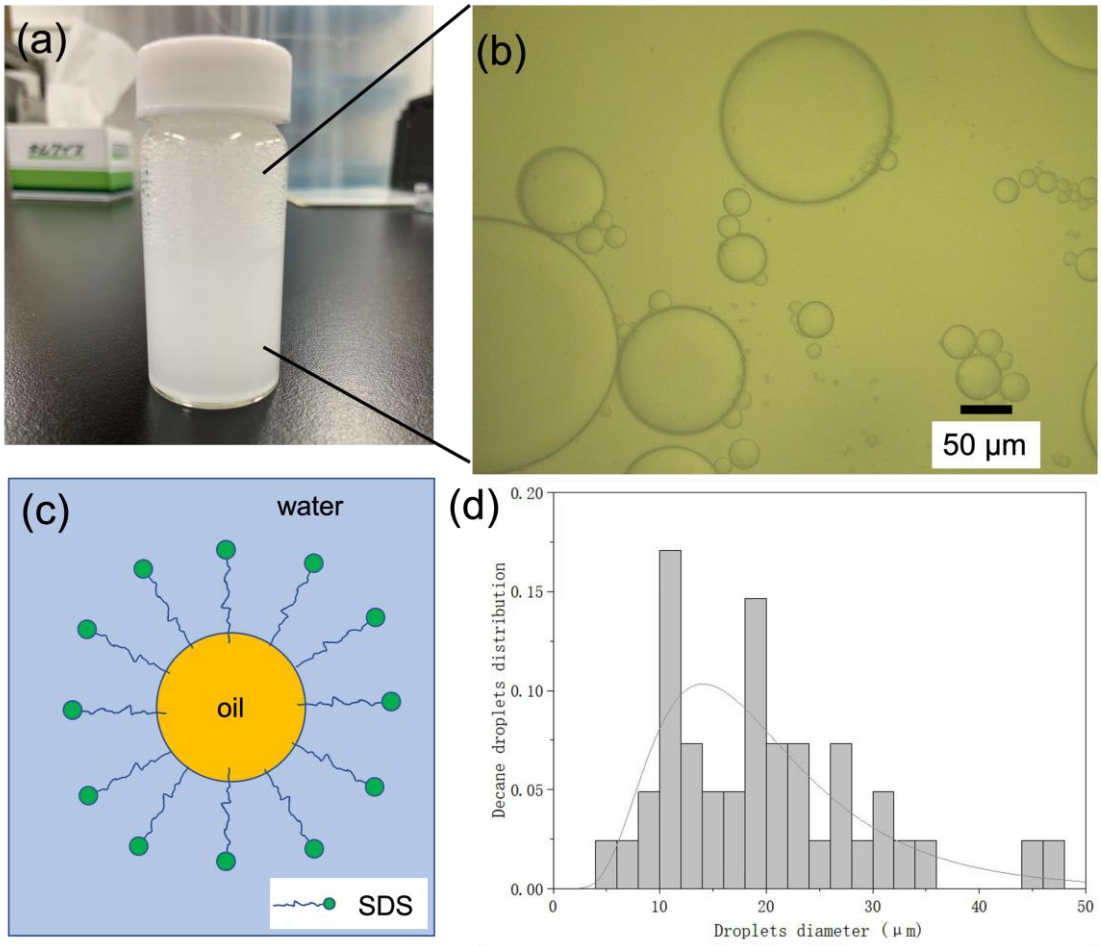

Figure 4-1. The oil-in water emulsion. (a) The image of emulsion. (b) The optical microscope image of emulsion. (c) The schematic of SDS in emulsion. (d) The distribution of decane droplets in emulsion.

Sodium dodecyl sulfate (SDS) is a water-soluble surfactant (HLB=40) that can be used to produce oil-in-water emulsions. The decane-in-water emulsions

were prepared by mixing decane and de-ion in 1:9 (v/v) with addition of 1.01wt% of SDS under magnetic stirring at high speed for 2 h. (Figure 4-1 (a))

The prepared emulsion with SDS is milky white due to the existence of emulsified oil droplets. And from Figure 4-1(b), (d), the oil droplets size as small as several microns to tens of microns, and just show the oil droplets distribution with the diameter from 3 to 50μm.

4.2 OIL-IN-WATER EMULSION SEPARATION WITH PB45

For oil-in-water emulsion separation, a water removing method is required. The Therefore, The PB45 is selected for oil-in-water separation. The PB45 prewetted by water first and cast the emulsion. From the Figure 4-2, after separation, since there are almost no micron-sized oil droplets, the filtrate becomes transparent.

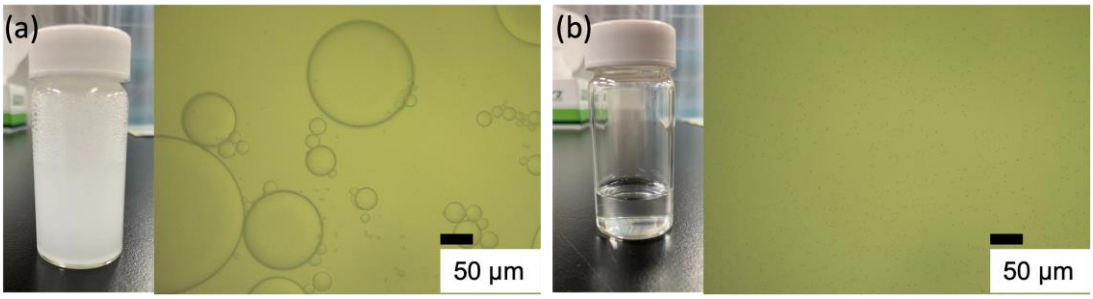

Figure 4-2. Photo and optical microscope images of emulsion (a) Before and (b) after the oil-in water emulsion

The separation principle is also to form a water lubricating layer prewetted by water, and then separate the oil-in-water emulsion with water removing method.

The flux of the separation of oil-in-water emulsion is about 150 $Lm^{-2}h^{-1}$. The separation rate is somewhat higher compared to other separation membranes under gravity systems. [142-144] These benefits from the uniform pore size of the honeycomb membrane, resulting in high porosity as well as mean pore size close to the largest pore size.

Table 4-1. The flux with different membranes separation oil-in-water by gravity.

	Flux ($Lm^{-2} h^{-1}$)	oil : water	Ø	pressure	Ref.
PB45 HC	>150	1:10	10μm	gravity	this work
TiO2/sulfonated graphene oxide/Ag	53	1:10	28μm	gravity	[136]
PA6(3)T fiber membrane	44.3	1:15	~122nm	gravity	[137]
PDA/PEI coating membrane	~120	1:100	no specific value 0.2μm	gravity	[138]

The separation rate is somewhat higher compared to other separation membranes under gravity systems. [142-144] Due to the uniform pore size of the honeycomb membrane, it has high porosity as well as mean pore size close to the largest pore size.

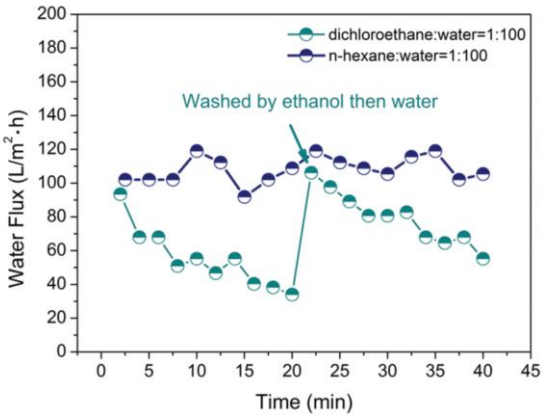

Figure 4-3. Water flux of dichloroethane-in-water (1 : 100, v/v) and *n*-hexane-in-water emulsion separation (1 : 100, v/v) with PDA/PEI-decorated membrane. [138] (Reproduced with permission, Copyright 2014 Royal Society of Chemistry)

Under the same conditions, the separation speed of the emulsion will be lower than that of the oil-water mixture. For emulsion separation membranes, the separation efficiency decreases with water removal. This is because the oil droplets are evenly dispersed in the emulsion, and some of the oil droplets will also contact the membrane at the bottom of the liquid. In addition, as the water flows downward through the membrane, a part of the oil droplets will also move to the bottom of the liquid. These will decrease the separation efficiency.

Suction filtration is a procedure in which a pressure differential is maintained across the filter medium by evacuating the air below the filter. The main advantage in using this type of filtration is that it proceeds much more quickly (several orders of magnitude) than simply allowing the liquid to drain through the filter medium via the force of gravity.

But if the pressure difference is too large, it may allow all the liquid to penetrate the porous membrane. And the pressure difference should lower than intrusion pressure. The capillary force of the permeation channels would provide an upward intrusion pressure ($\Delta P_{the} = \frac{2\gamma_{OW}\cos\theta_{OW}}{d}$ as mentioned before). Therefore, additional pressure can be applied under the premise that the total pressure is less than ΔP_{the}。 For PB45, the $\Delta P_{the} = 9.6kPa$ which could hold higher than 1 m decane on the membrane in gravity driven system. From the equation, further increasing the underwater oleophobicity of the films and reducing the pore size could increase the upper limit of the acceptable pressure. In addition, the PB membrane could also break if the pressure difference is too high. The tension strength of PB is about 10Mpa. However, the strength of the porous membrane will definitely decrease, and the UV-O_3 treatment will also reduce the tensile strength of the PB. So, if the separation efficiency under pressure is to be measured future, the tensile strength of the PB45 needs to be measured.

4.3 EXPERIMENTAL

4.3.1 FABRICATION OF PERFORATED PB45 MEMBRANE

PB (RB820) was kindly provided by JSR (Japan), and chloroform was purchased from Sigma-Aldrich (St. Louis, MO) and Fujifilm Wako Chemicals (Osaka, Japan). An amphiphilic copolymer (polymer 1, Mw= 40 kg mol^{-1}) was synthesized according to the method reported in the literature. HC-patterned films were prepared by depositing a 10–20 mL of 1–2 g L^{-1} chloroform solution of PB and polymer 1 (weight ratio PB/polymer 1 = 10:1) onto a PET substrate (10 × 30 cm2) under humid conditions (relative humidity≈90% and velocity 130 L min^{-1}) and ambient temperature. The film was then removed using isopropanol (EP/Fujifilm Wako Chemical Industry) and tweezers and transferred onto a PET mesh (SAN1260, Sanplatec, Osaka).

A UV–O_3 cleaner (OC-250615-D+A; Iwasaki Denki, Tokyo) was used for the hydrophilic treatment of the films. As-prepared HC films were placed in the exposure chamber and treated with UV–O3 for 45min at ambient temperature and pressure.

4.3.2 PREPARATION OF OIL-IN-WATER EMULSION

Decane (Fujifilm Wako Pure Chemical Industries) was chosen for the oil phase. First, 0.1g Sodium Dodecyl Sulfate (Fujifilm Wako Pure Chemical Industries) was added into deionized water, and then the decane was mixed into the mixture. The volume ratio of oil and water phases was 1:9. The oil-in-water emulsion was obtained after stirring quickly for 2 h with the high-speed shaker (ASCM-1, AS ONE, Osaka). The emulsion was examined using an optical microscope (VHX-500, Keyence, Osaka)

4.3.3. OIL-IN-WATER SEPARATION EXPERIMENTS

Decane (Fujifilm Wako Pure Chemical Industries) whose densities (ρo) are less than that of water (ρw), respectively, were used for the experiment. The mesh-reinforced HC film was fixed onto a funnel with a glass filter as a filter membrane

and was sandwiched with a glass cup with a clamp. Oil-in-water emulsion was poured from the top of the filter, and the liquid transported though the membrane was monitored using a video camera.

CHAPTER 5. CONCLUSION

In this thesis, I successfully prepared perforated honeycomb films with different wettability. The PB45 with the superhydrophilicity (water contact angle 0°) and superoleophilicity (oil contact angle 0°) could separate both oil-water mixture and oil-in-water emulsion.

In CHAPTER 2, when studying the wettability of different honeycomb films, the new droplets generation from the HC film was observed for the first time. By dyeing the decane droplet red, it can be judged that the new droplets generation from hydrophobic honeycomb films are air bubbles.

Another novel phenomenon is that the decane contact angle is about 154° underwater, but the decane can be absorbed. Calculated by spreading coefficient and Laplace pressure equations, the decane cannot spread on the underwater oleophobic surface. I think this is a very important point, that a surface with a high oil contact angle underwater does not necessarily repel oil vertically underwater and can still allow oil to pass through the porous structure.

Also, when studying the wettability of different honeycomb films, it can be clearly seen that the transparency has changed. By comparison, small changes in pore size had little effect on transparency. Large changes in wettability (from hydrophobic to superhydrophilic) also have little effect on transparency in air which shows from another perspective that after 60 min of UV-O_3 treatment, the structure of the honeycomb film has not changed. But the transparency of superhydrophilic honeycomb and pincushion structure films have significant increasing underwater. Along with the increase in transparency is the oleophobicity, which both indicates the lubricating layer forming with the replacement of air in the pores by water.

IN CHAPTER 3, after the UV-O_3 treatment, the honeycomb films cannot be transferred from the substrate, so the films are transferred from the substrate first, and then treated with UV-O_3.

For oil-water mixture separation, the PB and PB15 with hydrophobicity and oleophilicity successfully separated oil-water mixture with oil removing method.

the PB45 with controlled wettability can be used in membranes that can separate different liquids according to their densities when the initial liquid added to the surface of the HC film is changed. The thickness of the penetrated HC film is only a few micrometers, and it is surprising that a very thin film can separate liquid volumes on the order of tens of milliliters and the theoretical height of decane hold on PB45 is up to 1.34m.

The PB30 is hydrophobic but can also let the water pass through. Depending on this, I have studied the process of the gradual transition from the Cassie model to the Wenzel model and find the penetration condition of honeycomb films is $\cos\Theta_{w/a-flat} > \frac{1-\emptyset_{polymer}}{r-\emptyset_{polymer}}$.

The calculation of the penetration condition requires the flat films contact angle. I found that, increasing roughness turns hydrophilic material to hydrophobic surface. Other researchers indicate that the limit for hydrophilic materials is 65°. And in this study, the flat surface with 28° could also change to hydrophobic surface with the honeycomb structure because of the high barrier energy.

In CHAPTER 4, the PB45 can also separate oil-in-water emulsions just in gravity-driven system. When the ratio of oil to water is about 1:10, the separation efficiency is better than other emulsion separation membranes in gravity-driven system.

In this thesis is the first success of the UV-O_3 treated lubricated Honeycomb (HC) Films for sufficient oil-water mixture and oil-in-water emulsion separation membranes with gravity-driven system and also proposed novel insight of the phenomena and mechanism.

REFERENCE

[1] Cheryan, M., and N. Rajagopalan. "Membrane processing of oily streams. Wastewater treatment and waste reduction." *Journal of membrane science* 151.1 **(1998)**: 13-28.

[2] Garcıa-Sánchez, A., and E. Alvarez-Ayuso. "Sorption of Zn, Cd and Cr on calcite. Application to purification of industrial wastewaters." *Minerals Engineering* 15.7 **(2002)**: 539-547.

[3] Gatsios, Evangelos, John N. Hahladakis, and Evangelos Gidarakos. "Optimization of electrocoagulation (EC) process for the purification of a real industrial wastewater from toxic metals." *Journal of Environmental Management* 154 **(2015)**: 117-127.

[4] Ani, J. U., et al. "Nephelometric and functional parameters response of coagulation for the purification of industrial wastewater using Detarium microcarpum." *Journal of hazardous materials* 243 **(2012)**: 59-66.

[5] Anisuddin, S., Al Hashar, N., & Tahseen, S. **(2005)**. PREVENTION OF OIL SPILL POLLUTION IN SEAWATER USING LOCALLY AVAILABLE MATERIALS. *Arabian Journal for Science & Engineering (Springer Science & Business Media BV)*, *30*.

[6] Sarbatly, Rosalam, Duduku Krishnaiah, and Zykamilia Kamin. "A review of polymer nanofibres by electrospinning and their application in oil–water separation for cleaning up marine oil spills." *Marine pollution bulletin* 106.1-2 **(2016)**: 8-16.

[7] Gupta, Raju Kumar, et al. "Oil/water separation techniques: a review of recent progresses and future directions." *Journal of Materials Chemistry A* 5.31 **(2017)**: 16025-16058.

[8] Liu, Qin, et al. "Recent advances in energy materials by electrospinning." *Renewable and Sustainable Energy Reviews* 81 **(2018)**: 1825-1858.

[9] Alvarez, Pedro JJ, et al. "Emerging opportunities for nanotechnology to enhance water security." *Nature nanotechnology* 13.8 **(2018)**: 634-641.

[10] Zhu, Liangliang, et al. "Recent progress in solar-driven interfacial water evaporation: Advanced designs and applications." *Nano Energy* 57 **(2019)**: 507-518.

[11] Kuang, Yudi, et al. "A high-performance self-regenerating solar evaporator for continuous water desalination." *Advanced materials* 31.23 **(2019)**: 1900498.

[12] Jiang, Kun, et al. "Highly selective oxygen reduction to hydrogen peroxide on transition metal single atom coordination." *Nature communications* 10.1 **(2019)**: 1-11.

[13] Benito, JoséManuel, et al. "Design and construction of a modular pilot plant for the treatment of oil-containing wastewaters." *Desalination* 147.1-3 **(2002)**: 5-10.

[14] Husseien, M., et al. "A comprehensive characterization of corn stalk and study of carbonized corn stalk in dye and gas oil sorption." *Journal of Analytical and Applied Pyrolysis* 86.2 **(2009)**: 360-363.

[15] Fritt-Rasmussen, Janne, Susse Wegeberg, and Kim Gustavson. "Review on burn residues from in situ burning of oil spills in relation to Arctic waters." *Water, Air, & Soil Pollution* 226.10 **(2015)**: 1-12.

[16] Bullock, Robin J., Robert A. Perkins, and Srijan Aggarwal. "In-situ burning with chemical herders for Arctic oil spill response: Meta-analysis and review." *Science of the Total Environment* 675 **(2019)**: 705-716.

[17] Lessard, Richard R., and Greg DeMarco. "The significance of oil spill dispersants." *Spill Science & Technology Bulletin* 6.1 **(2000)**: 59-68.

[18] Chapman, Helen, et al. "The use of chemical dispersants to combat oil spills at sea: A review of practice and research needs in Europe." *Marine Pollution Bulletin* 54.7 **(2007)**: 827-838.

[19] Schaflinger, Uwe. "Centrifugal separation of a mixture." *Fluid Dynamics Research* 6.5-6 **(1990)**: 213.

[20] Wang, Xianfeng, et al. "Electrospun nanofibrous materials: a versatile medium for effective oil/water separation." *Materials today* 19.7 **(2016)**: 403-414.

[21] SPCC GUIDANCE FOR REGIONAL INSPECTORS, December 16, **2013**

[22] Gaaseidnes, Knut, and Joseph Turbeville. "Separation of oil and water in oil spill recovery operations." *Pure and applied chemistry* 71.1 **(1999)**: 95-101.

[23] Frising, Tom, Christine Noïk, and Christine Dalmazzone. "The liquid/liquid sedimentation process: from droplet coalescence to technologically enhanced water/oil emulsion gravity separators: a review." *Journal of dispersion science and technology* 27.7 **(2006)**: 1035-1057.

[24] Xu, Jiajie, et al. "In-line and selective phase separation of medium-chain carboxylic acids using membrane electrolysis." *Chemical Communications* 51.31 **(2015)**: 6847-6850.

[25] Deng, Yuying, et al. "Recent development of super-wettable materials and their applications in oil-water separation." *Journal of Cleaner Production* 266 **(2020)**: 121624.

[26] Padaki, Mahesh, et al. "Membrane technology enhancement in oil–water separation. A review." *Desalination* 357 **(2015)**: 197-207.

[27] Gupta, Raju Kumar, et al. "Oil/water separation techniques: a review of recent progresses and future directions." *Journal of Materials Chemistry A* 5.31 **(2017)**: 16025-16058.

[28] Wei, Yibin, et al. "Specially wettable membranes for oil–water separation." *Advanced Materials Interfaces* 5.23 **(2018)**: 1800576.

[29] Yue, Xuejie, et al. "Design and fabrication of superwetting fiber-based membranes for oil/water separation applications." *Chemical Engineering Journal* 364 **(2019)**: 292-309.

[30] Qiu, Lei, Yihan Sun, and Zhiguang Guo. "Designing novel superwetting surfaces for high-efficiency oil–water separation: design principles, opportunities, trends and challenges." *Journal of Materials Chemistry A* 8.33 **(2020)**: 16831-16853.

[31] Deng, Yuying, et al. "Metal-organic framework membranes: Recent development in the synthesis strategies and their application in oil-water separation." *Chemical Engineering Journal* 405 **(2021)**: 127004.

[32] Rasouli, Seyedabbas, et al. "Superhydrophobic and superoleophilic membranes for oil-water separation application: A comprehensive review." *Materials & Design* 204 **(2021)**: 109599.

[33] Lin, Xiangde, and Jinkee Hong. "Recent advances in robust superwettable membranes for oil–water separation." *Advanced Materials Interfaces* 6.12 **(2019)**: 1900126.

[34] Junaidi, Nurul Fattin Diana, et al. "Recent development of graphene oxide-based membranes for oil–water separation: A review." *Separation and Purification Technology* 258 **(2021)**: 118000.

[35] Ma, Wenjing, et al. "Electrospun fibers for oil–water separation." *Rsc Advances* 6.16 **(2016)**: 12868-12884.

[36] Ryu, Ji Hyun, Seonki Hong, and Haeshin Lee. "Bio-inspired adhesive catechol-conjugated chitosan for biomedical applications: A mini review." *Acta biomaterialia* 27 **(2015)**: 101-115.

[37] Marmur, Abraham. "The lotus effect: superhydrophobicity and metastability." *Langmuir* 20.9 **(2004)**: 3517-3519.

[38] Rahim, Md Arifur, et al. "Phenolic building blocks for the assembly of functional materials." *Angewandte Chemie International Edition* 58.7 **(2019)**: 1904-1927.

[39] Xu, Li Qun, Koon-Gee Neoh, and En-Tang Kang. "Natural polyphenols as versatile platforms for material engineering and surface functionalization." *Progress in Polymer Science* 87 **(2018)**: 165-196.

[40] McKittrick, J., et al. "Energy absorbent natural materials and bioinspired design strategies: a review." *Materials Science and Engineering: C* 30.3 **(2010)**: 331-342.

[41] Chen, Ke, et al. "Binary synergy strengthening and toughening of bio-inspired nacre-like graphene oxide/sodium alginate composite paper." *Acs Nano* 9.8 **(2015)**: 8165-8175.

[42] San Ha, Ngoc, and Guoxing Lu. "A review of recent research on bio-inspired structures and materials for energy absorption applications." *Composites Part B: Engineering* 181 **(2020)**: 107496.

[43] Kar, Arpan Kumar. "Bio inspired computing–a review of algorithms and scope of applications." *Expert Systems with Applications* 59 **(2016)**: 20-32.

[44] Tadepalli, Sirimuvva, et al. "Bio-optics and bio-inspired optical materials." *Chemical reviews* 117.20 **(2017)**: 12705-12763.

[45] Marmur, Abraham. "The lotus effect: superhydrophobicity and metastability." *Langmuir* 20.9 **(2004)**: 3517-3519.

[46] Banerjee, Indrani, Ravindra C. Pangule, and Ravi S. Kane. "Antifouling coatings: recent developments in the design of surfaces that prevent fouling by proteins, bacteria, and marine organisms." *Advanced materials* 23.6 **(2011)**: 690-718.

[47] Parvate, Sumit, Prakhar Dixit, and Sujay Chattopadhyay. "Superhydrophobic surfaces: insights from theory and experiment." *The Journal of Physical Chemistry B* 124.8 **(2020)**: 1323-1360.

[48] Wei, David W., et al. "Superhydrophobic modification of cellulose and cotton textiles: Methodologies and applications." *Journal of Bioresources and Bioproducts* 5.1 **(2020)**: 1-15.

[49] Shi, Feng, et al. "Towards understanding why a superhydrophobic coating is needed by water striders." *Advanced Materials* 19.17 **(2007)**: 2257-2261.

[50] Wang, Shutao, et al. "Bioinspired surfaces with superwettability: new insight on theory, design, and applications." *Chemical reviews* 115.16 **(2015)**: 8230-8293.

[51] Darmanin, Thierry, and Frédéric Guittard. "Superhydrophobic and superoleophobic properties in nature." *Materials today* 18.5 **(2015)**: 273-285.

[52] Ivanova, Elena P., et al. "Antifungal versus antibacterial defence of insect wings." *Journal of Colloid and Interface Science* 603 **(2021)**: 886-897.

[53] Dizge, Nadir, Evyatar Shaulsky, and Vasiliki Karanikola. "Electrospun cellulose nanofibers for superhydrophobic and oleophobic membranes." *Journal of Membrane Science* 590 **(2019)**: 117271.

[54] Wang, Chenghong, and Zhiguang Guo. "A comparison between superhydrophobic surfaces (SHS) and slippery liquid-infused porous surfaces (SLIPS) in application." *Nanoscale* 12.44 **(2020)**: 22398-22424.

[55] Zdziennicka, Anna, et al. "Some remarks on the solid surface tension determination from contact angle measurements." *Applied Surface Science* 405 (2017): 88-101.

[56] Ross, Sydney, and Paul Becher. "The history of the spreading coefficient." *Journal of colloid and interface science* 149.2 **(1992)**: 575-579.

[57] Schrader, Malcolm E. "Young-dupre revisited." *Langmuir* 11.9 **(1995)**: 3585-3589.

[58] Wenzel, Robert N. "Resistance of solid surfaces to wetting by water." *Industrial & Engineering Chemistry* 28.8 **(1936)**: 988-994.

[59] Cassie, A. B. D., and SJToTFS Baxter. "Wettability of porous surfaces." *Transactions of the Faraday society* 40 **(1944)**: 546-551.

[60] Feng, Lin, et al. "A super-hydrophobic and super-oleophilic coating mesh film for the separation of oil and water." *Angewandte Chemie* 116.15 **(2004)**: 2046-2048.

[61] Zhou, Xiaoyan, et al. "Robust and durable superhydrophobic cotton fabrics for oil/water separation." *ACS applied materials & interfaces* 5.15 **(2013)**: 7208-7214.

[62] Xue, Chao-Hua, et al. "Fabrication of superhydrophobic and superoleophilic textiles for oil–water separation." *Applied Surface Science* 284 **(2013)**: 464-471.

[63] Crick, Colin R., James A. Gibbins, and Ivan P. Parkin. "Superhydrophobic polymer-coated copper-mesh; membranes for highly efficient oil–water separation." *Journal of Materials Chemistry A* 1.19 **(2013)**: 5943-5948.

[64] Gao, Xin, et al. "Robust superhydrophobic foam: a graphdiyne-based hierarchical architecture for oil/water separation." *Advanced Materials* 28.1 **(2016)**: 168-173.

[65] Li, Jian, et al. "Superhydrophobic meshes that can repel hot water and strong corrosive liquids used for efficient gravity-driven oil/water separation." *Nanoscale* 8.14 **(2016)**: 7638-7645.

[66] Zhou, Cailong, et al. "Nature-inspired strategy toward superhydrophobic fabrics for versatile oil/water separation." *ACS applied materials & interfaces* 9.10 **(2017)**: 9184-9194.

[67] Zhang, Zhi-hui, et al. "One-step fabrication of robust superhydrophobic and superoleophilic surfaces with self-cleaning and oil/water separation function." *Scientific reports* 8.1 **(2018)**: 1-12.

[68] Zhu, Xiaoying, et al. "Effective and low fouling oil/water separation by a novel hollow fiber membrane with both hydrophilic and oleophobic surface properties." *Journal of membrane science* 466 **(2014)**: 36-44.

[69] Adewunmi, Ahmad A., and Muhammad Shahzad Kamal. "Effect of water/decane ratios and salt on the stability, rheology, and interfacial tension of water/decane emulsions." *Energy & Fuels* 33.9 **(2019)**: 8456-8462.

[70] Ikhsan, Syarifah Nazirah Wan, et al. "Superwetting materials for hydrophilic-oleophobic membrane in oily wastewater treatment." *Journal of Environmental Management* 290 **(2021)**: 112565.

[71] Wong, Tak-Sing, et al. "Bioinspired self-repairing slippery surfaces with pressure-stable omniphobicity." *Nature* 477.7365 **(2011)**: 443-447.

[72] Vogel, Nicolas, et al. "Transparency and damage tolerance of patternable omniphobic lubricated surfaces based on inverse colloidal monolayers." *Nature communications* 4.1 **(2013)**: 1-10.

[73] Waghmare, Prashant R., Naga Siva Kumar Gunda, and Sushanta K. Mitra. "Under-water superoleophobicity of fish scales." *Scientific reports* 4.1 **(2014)**: 1-5.

[74] Chen, Chaolang, et al. "Separation mechanism and construction of surfaces with special wettability for oil/water separation." *ACS applied materials & interfaces* 11.11 **(2019)**: 11006-11027.

[75] Liu, Mingjie, et al. "Bioinspired design of a superoleophobic and low adhesive water/solid interface." *Advanced Materials* 21.6 **(2009)**: 665-669.

[76] Wang, Yonghua, et al. "One-step method using laser for large-scale preparation of bionic superhydrophobic & drag-reducing fish-scale surface." *Surface and Coatings Technology* 409 **(2021)**: 126801.

[77] He, Huaqiang, et al. "Superhydrophilic fish-scale-like CuC2O4 nanosheets wrapped copper mesh with underwater super oil-repellent properties for effective separation of oil-in-water emulsions." *Colloids and Surfaces A: Physicochemical and Engineering Aspects* 627 **(2021)**: 127133.

[78] Su, Xin, et al. "Design of hierarchical comb hydrophilic polymer brush (HCHPB) surfaces inspired by fish mucus for anti-biofouling." *Journal of Materials Chemistry B* 7.8 **(2019)**: 1322-1332.

[79] Yong, Jiale, et al. "A review of femtosecond laser-structured superhydrophobic or underwater superoleophobic porous surfaces/materials for efficient oil/water separation." *RSC advances* 9.22 **(2019)**: 12470-12495.

[80] Zhao, Siyang, et al. "A robust surface with superhydrophobicity and underwater superoleophobicity for on-demand oil/water separation." *Nanoscale* 13.36 **(2021)**: 15334-15342.

[81] Cheng, Zhongjun, et al. "pH-controllable on-demand oil/water separation on the switchable superhydrophobic/superhydrophilic and underwater low-adhesive superoleophobic copper mesh film." *Langmuir* 31.4 **(2015)**: 1393-1399.

[82] Gou, Xiaodan, et al. "Superhydrophilic and underwater superoleophobic cement-coated mesh for oil/water separation by gravity." *Colloids and Surfaces A: Physicochemical and Engineering Aspects* 605 **(2020)**: 125338.

[83] Wang, Meng, et al. "Mussel-inspired chitosan modified superhydrophilic and underwater superoleophobic cotton fabric for efficient oil/water separation." *Carbohydrate polymers* 244 **(2020)**: 116449.

[84] Zeng, Zhi-wei Steven, and Spencer E. Taylor. "Facile preparation of superhydrophobic melamine sponge for efficient underwater oil-water separation." *Separation and Purification Technology* 247 **(2020)**: 116996.

[85] Kavalenka, M. N., et al. "Wood-based microhaired superhydrophobic and underwater superoleophobic surfaces for oil/water separation." *Rsc Advances* 4.59 **(2014)**: 31079-31083.

[86] Zeng, Minxiang, et al. "Highly biocompatible, underwater superhydrophilic and multifunctional biopolymer membrane for efficient oil–water separation and aqueous pollutant removal." *ACS Sustainable Chemistry & Engineering* 6.3 **(2018)**: 3879-3887.

[87] Zhu, Meng, et al. "Robust superhydrophilic and underwater superoleophobic membrane optimized by Cu doping modified metal-organic frameworks for oil-water separation and water purification." *Journal of Membrane Science* 640 **(2021)**: 119755.

[88] Wang, Jiaqi, et al. "Reversible wettability between underwater superoleophobicity and superhydrophobicity of stainless steel mesh for efficient oil–water separation." *ACS omega* 6.1 **(2020)**: 77-84.

[89] Widawski, Gilles, Michel Rawiso, and Bernard François. "Self-organized honeycomb morphology of star-polymer polystyrene films." *Nature* 369.6479 **(1994)**: 387-389.

[90] Yabu, Hiroshi, Kouta Inoue, and Masatsugu Shimomura. "Multiple-periodic structures of self-organized honeycomb-patterned films and polymer nanoparticles hybrids." *Colloids and Surfaces A: Physicochemical and Engineering Aspects* 284 **(2006)**: 301-304.

[91] Chen, Bihai, Takehiko Wada, and Hiroshi Yabu. "Amphiphilic Perforated Honeycomb Films for Gravimetric Liquid Separation." *Advanced Materials Interfaces* 9.1 **(2022)**: 2101954.

[92] Yabu, Hiroshi, and Masatsugu Shimomura. "Mesoscale pincushions, microrings, and microdots prepared by heating and peeling of self-organized honeycomb-patterned films deposited on a solid substrate." *Langmuir* 22.11 **(2006)**: 4992-4997.

[93] Chen, Bihai, Takehiko Wada, and Hiroshi Yabu. "Underwater Bubble and Oil Repellency of Biomimetic Pincushion and Plastron-Like Honeycomb Films." *Langmuir* 36.23 **(2020)**: 6365-6369.

[94] Yabu, Hiroshi, et al. "Self-assembled porous templates allow pattern transfer to poly (dimethyl siloxane) sheets through surface wrinkling." *Polymer journal* 44.6 **(2012)**: 573-578.

[95] Yamazaki, Hidekazu, et al. "Formation and control of line defects caused by tectonics of water droplet arrays during self-organized honeycomb-patterned polymer film formation." *Soft Matter* 10.16 **(2014)**: 2741-2747.

[96] Yabu, Hiroshi, and Masatsugu Shimomura. "Single-step fabrication of transparent superhydrophobic porous polymer films." *Chemistry of materials* 17.21 **(2005)**: 5231-5234.

[97] Yabu, Hiroshi, et al. "Superhydrophobic and lipophobic properties of self-organized honeycomb and pincushion structures." *Langmuir* 21.8 **(2005)**: 3235-3237.

[98] Kamei, Jun, and Hiroshi Yabu. "On-Demand Liquid Transportation Using Bioinspired Omniphobic Lubricated Surfaces Based on Self-Organized Honeycomb and Pincushion Films." *Advanced Functional Materials* 25.27 **(2015)**: 4195-4201.

[99] Kamei, Jun, and Hiroshi Yabu. "One step fabrication of mesh-reinforced hierarchic perforated microporous honeycomb films with tunable filtering property." *Soft Matter* 13.43 **(2017)**: 7834-7839.

[100] El-Samak, Ali A., et al. "Designing flexible and porous fibrous membranes for oil water separation—A review of recent developments." *Polymer Reviews* 60.4 **(2020)**: 671-716.

[101] Dunne, R., D. Desai, and R. Sadiku. "A review of the factors that influence sound absorption and the available empirical models for fibrous materials." *Acoustics Australia* 45.2 **(2017)**: 453-469.

[102] Fan, Tingting, et al. "Robust graphene@ PPS fibrous membrane for harsh environmental oil/water separation and all-weather cleanup of crude oil spill by joule heat and photothermal effect." *ACS Applied Materials & Interfaces* 13.16 **(2021)**: 19377-19386.

[103] Cheng, Qiaoyun, et al. "Facile fabrication of superhydrophilic membranes consisted of fibrous tunicate cellulose nanocrystals for highly efficient oil/water separation." *Journal of Membrane Science* 525 **(2017)**: 1-8.

[104] Wang, Antuo, et al. "A tree-grapes-like PTFE fibrous membrane with super-hydrophobic and durable performance for oil/water separation." *Separation and Purification Technology* 275 **(2021)**: 119165.

[105] Xu, Ying, Baoku Zhu, and Youyi Xu. "A study on formation of regular honeycomb pattern in polysulfone film." *Polymer* 46.3 **(2005)**: 713-717.

[106] Yin, Ming-Jie, et al. "Precise micropatterning of a porous poly (ionic liquid) via maskless photolithography for high-performance nonenzymatic H2O2 sensing." *ACS nano* 12.12 **(2018)**: 12551-12557.

[107] Pratiwi, Nuraini Dian, et al. "Fabrication of porous silicon using photolithography and reactive ion etching (RIE)." *Materials Today: Proceedings* 13 **(2019)**: 92-96.

[108] Lorrain, Nathalie, et al. "Submicron gap reduction of micro-resonator based on porous silica ridge waveguides manufactured by standard photolithographic process." *Optical Materials* 88 **(2019)**: 210-217.

[109] Hu, Yang, et al. "Surface engineering of spongy bacterial cellulose via constructing crossed groove/column micropattern by low-energy CO2 laser photolithography toward scar-free wound healing." *Materials Science and Engineering: C* 99 **(2019)**: 333-343.

[110] Li, Tingjie, et al. "Self-detached membranes with well-defined pore size, shape and distribution fabricated by underexposure photolithography." *Journal of Vacuum Science & Technology B, Nanotechnology and Microelectronics: Materials, Processing, Measurement, and Phenomena* 38.4 **(2020)**: 042601.

[111] Oliveira Jr, Osvaldo N., Luciano Caseli, and Katsuhiko Ariga. "The past and the future of Langmuir and Langmuir–Blodgett films." *Chemical Reviews* 122.6 **(2022)**: 6459-6513.

[112] Hussain, Syed Arshad, et al. "Unique supramolecular assembly through Langmuir–Blodgett (LB) technique." *Heliyon* 4.12 **(2018)**: e01038.

[113] Baratto, Camilla, et al. "On the alignment of ZnO nanowires by Langmuir–Blodgett technique for sensing application." *Applied Surface Science* 528 **(2020)**: 146959.

[114] Chiu, Yu-Cheng, et al. "Highly ordered luminescent microporous films prepared from crystalline conjugated rod-coil diblock copolymers of PF-b-PSA and their superhydrophobic characteristics." *Soft Matter* 7.19 **(2011)**: 9350-9358.

[115] Patankar, Neelesh A. "Supernucleating surfaces for nucleate boiling and dropwise condensation heat transfer." *Soft Matter* 6.8 **(2010)**: 1613-1620.

[116] Kharangate, Chirag R., and Issam Mudawar. "Review of computational studies on boiling and condensation." *International Journal of Heat and Mass Transfer* 108 **(2017)**: 1164-1196.

[117] Beysens, D., et al. "How does dew form?." *Phase Transitions* 31.1-4 **(1991)**: 219-246.

[118] Fukuhira, Yukako, et al. "Interfacial tension governs the formation of self-organized honeycomb-patterned polymer films." *Soft Matter* 5.10 **(2009)**: 2037-2041.

[119] Fukuhira, Yukako, et al. "Biodegradable honeycomb-patterned film composed of poly (lactic acid) and dioleoylphosphatidylethanolamine." *Biomaterials* 27.9 **(2006)**: 1797-1802.

[120] Kawano, Takahito, et al. "Honeycomb-shaped surface topography induces differentiation of human mesenchymal stem cells (hMSCs): Uniform porous polymer scaffolds prepared by the breath figure technique." *Biomaterials science* 2.1 **(2014)**: 52-56.

[121] Bui, Van-Tien, Seung Hyeon Ko, and Ho-Suk Choi. "A surfactant-free bio-compatible film with a highly ordered honeycomb pattern fabricated via an improved phase separation method." *Chemical Communications* 50.29 **(2014)**: 3817-3819.

[122] Yabu, Hiroshi, Kouta Inoue, and Masatsugu Shimomura. "Multiple-periodic structures of self-organized honeycomb-patterned films and polymer nanoparticles hybrids." *Colloids and Surfaces A: Physicochemical and Engineering Aspects* 284 **(2006)**: 301-304.

[123] Kamei, Jun, Hiroya Abe, and Hiroshi Yabu. "Biomimetic bubble-repellent tubes: Microdimple arrays enhance repellency of bubbles inside of tubes." *Langmuir* 33.2 **(2017)**: 585-590.

[124] Yong, Jiale, et al. "Bioinspired transparent underwater superoleophobic and anti-oil surfaces." *Journal of Materials Chemistry A* 3.18 **(2015)**: 9379-9384.

[125] Ruffolo, Silvestro A., et al. "Antifouling coatings for underwater archaeological stone materials." *Progress in Organic Coatings* 104 **(2017)**: 64-71.

[126] Del Grosso, Chelsey A., et al. "Surface hydration for antifouling and bio-adhesion." *Chemical Science* 11.38 **(2020)**: 10367-10377.

[127] Huo, Jinglan, et al. "Underwater transparent miniature “mechanical hand” based on femtosecond laser-induced controllable oil-adhesive patterned glass for oil droplet manipulation." *Langmuir* 33.15 **(2017)**: 3659-3665.

[128] Zhou, Cailong, et al. "Superhydrophilic and underwater superoleophobic titania nanowires surface for oil repellency and oil/water separation." *Chemical Engineering Journal* 301 **(2016)**: 249-256.

[129] Huynh, So Hung, et al. "Plastron-mediated growth of captive bubbles on superhydrophobic surfaces." *Langmuir* 31.24 **(2015)**: 6695-6703.

[130] Li, Zhe, et al. "A porous superhydrophobic surface with active air plastron control for drag reduction and fluid impalement resistance." *Journal of Materials Chemistry A* 7.27 **(2019)**: 16387-16396.

[131] Hirai, Yuji, Naoki Yanagi, and Masatsugu Shimomura. "Preparations of the artificial plastron device by self-organized honeycomb-patterned films." *e-Journal of Surface Science and Nanotechnology* 13 **(2015)**: 90-92.

[132] Lucas, Richard. "Ueber das Zeitgesetz des kapillaren Aufstiegs von Flüssigkeiten." *Kolloid-Zeitschrift* 23.1 **(1918)**: 15-22.

[133] Washburn, Edward W. "Note on a method of determining the distribution of pore sizes in a porous material." *Proceedings of the National Academy of Sciences* 7.4 **(1921)**: 115-116.

[134] Zhang, Feng, et al. "Nanowire-haired inorganic membranes with superhydrophilicity and underwater ultralow adhesive superoleophobicity for high-efficiency oil/water separation." *Advanced Materials* 25.30 **(2013)**: 4192-4198.

[135] Lafuma, Aurélie, and David Quéré. "Superhydrophobic states." *Nature materials* 2.7 **(2003)**: 457-460.

[136] Finn, Robert. "The contact angle in capillarity." *Physics of Fluids* 18.4 **(2006)**: 047102.

[137] Chen, Ting, et al. "Smart ZIF-L mesh films with switchable superwettability synthesized via a rapid energy-saving process." *Separation and Purification Technology* 240 **(2020)**: 116647.

[138] Zhou, Peizhang, et al. "Ultrafast preparation of hydrophobic ZIF-67/copper mesh via electrodeposition and hydrophobization for oil/water separation and dyes adsorption." *Separation and Purification Technology* 272 **(2021)**: 118871.

[139] Wen, Qiang, et al. "Zeolite-coated mesh film for efficient oil–water separation." *Chemical Science* 4.2 **(2013)**: 591-595.

[140] Li, Jian, et al. "Underwater superoleophobic palygorskite coated meshes for efficient oil/water separation." *Journal of materials chemistry A* 3.28 **(2015)**: 14696-14702.

[141] Griffin, William C. "Classification of surface-active agents by" HLB"." *J. Soc. Cosmet. Chem.* 1 **(1949)**: 311-326.

[142] Qian, Dongliang, et al. "TiO2/sulfonated graphene oxide/Ag nanoparticle membrane: In situ separation and photodegradation of oil/water emulsions." *Journal of membrane science* 554 **(2018)**: 16-25.

[143] Lin, Yi-Min, and Gregory C. Rutledge. "Separation of oil-in-water emulsions stabilized by different types of surfactants using electrospun fiber membranes." *Journal of membrane science* 563 **(2018)**: 247-258.

[144] Yang, Hao-Cheng, et al. "Mussel-inspired modification of a polymer membrane for ultra-high water permeability and oil-in-water emulsion separation." *Journal of Materials Chemistry A* 2.26 **(2014)**: 10225-10230.

ACKNOWLEDGEMENT

This study has been carried out under the guidance of Professor Takehiko Wada at The Institute of Multidisciplinary Research for Advanced Materials and Department of Chemistry, Graduate School of Science, Tohoku University And Professor Hiroshi Yabu at the Advanced Institute for Materials Research, Tohoku University.

I would like to greatly thank Professor Takehiko Wada for offering me the opportunity to study in this field with them guidance. His passion for science and life also deeply inspires me.

I would like to greatly thank Professor Hiroshi Yabu for giving me a lot of instructive comments on my research. And he always gave me careful guidance and enthusiastic help. When I encountered difficulties in the subject, it was the guidance of Professor Hiroshi Yabu, which enabled my research work to continue smoothly.

I would like to greatly thank Professor Akihide Hibara, Professor Seiichi Nishizawa, Professor Eriko Nango and Professor Hiroshi Kadokura for them critical advice to this thesis.

I would like to thank Dr. Manjit S. Grewal for his advices to this thesis.

I would like to thank technical staff Minori Suzuki for training me skills of multifarious experiments.

I would like to thank Mrs. Yoko Goto for taking care of the routine work.

I would like to thank my parents for supporting me to continue my studies after graduation whether mental or financial. During the toughest times, it was the unconditional support of my parents that allowed me to concentrate on my research.

I would like to thank my friends who have enriched my life and allowed me to relax and moderate my life.

I would like to thank all the people I meet here who made my life more interesting and enrichment.